AGU PUBLICATIONS

Tectonics

RESEARCH ARTICLE
10.1002/2014TC003618

Key Points:
- Structural and thermal studies of the El Oro metamorphic province
- Mesozoic evolution of the Ecuadorian fore arc

Supporting Information:
- Figures S1 and S2

Correspondence to:
N. Riel,
a.nicolas.riel@gmail.com

Citation:
Riel, N., J.-E. Martelat, S. Guillot, E. Jaillard, P. Monié, J. Yuquilema, G. Duclaux, and J. Mercier (2014), Fore arc tectonothermal evolution of the El Oro metamorphic province (Ecuador) during the Mesozoic, *Tectonics*, *33*, 1989–2012, doi:10.1002/2014TC003618.

Received 22 APR 2014
Accepted 19 SEP 2014
Accepted article online 23 SEP 2014
Published online 25 OCT 2014

Fore arc tectonothermal evolution of the El Oro metamorphic province (Ecuador) during the Mesozoic

Nicolas Riel[1], Jean-Emmanuel Martelat[2], Stéphane Guillot[1], Etienne Jaillard[1], Patrick Monié[3], Jonatan Yuquilema[4], Guillaume Duclaux[5], and Jonathan Mercier[1]

[1]ISTerre, IRD, Université Grenoble Alpes, CNRS, Grenoble, France, [2]Laboratoire de Géologie de Lyon, UCBL, ENS de Lyon, CNRS, Villeurbanne, France, [3]Université Montpellier, Géosciences Montpellier, Montpellier CEDEX 5, France, [4]Facultad de Geología y Petróleos, Escuela Politécnica Nacional, Quito, Ecuador, [5]CSIRO Earth Science and Resource Engineering, North Ryde, New South Wales, Australia

Abstract The El Oro metamorphic province of SW Ecuador is a composite massif made of juxtaposed terranes of both continental and oceanic affinity that has been located in a fore-arc position since Late Paleozoic times. Various geochemical, geochronological, and metamorphic studies have been undertaken on the El Oro metamorphic province, providing an understanding of the origin and age of the distinct units. However, the internal structures and geodynamic evolution of this area remain poorly understood. Our structural analysis and thermal modeling in the El Oro metamorphic province show that this fore-arc zone underwent four main geological events. (1) During Triassic times (230–225 Ma), the emplacement of the Piedras gabbroic unit at crustal-root level (~9 kbar) triggered partial melting of the metasedimentary sequence under an E-W extensional regime at pressure-temperature conditions ranging from 4.5 to 8.5 kbar and from 650 to 900°C for the migmatitic unit. (2) At 226 Ma, the tectonic underplating of the Arenillas-Panupalí oceanic unit (9 kbar and 300°C) thermally sealed the fore-arc region. (3) Around the Jurassic-Cretaceous boundary, the shift from trench-normal to trench-parallel subduction triggered the exhumation and underplating of the high-pressure, oceanic Raspas Ophiolitic Complex (18 kbar and 600°C) beneath the El Oro Group (130–120 Ma). This was followed by the opening of a NE-SW pull-apart basin, which tilted the massif along an E-W subhorizontal axis (110 Ma). (4) In Late Cretaceous times, an N-S compressional event generated heterogeneous deformation due to the presence of the Cretaceous Celica volcanic arc, which acted as a buttress and predominantly affected the central and eastern part of the massif.

1. Introduction

The South American margin has been the locus of plate convergence throughout much of the Phanerozoic [i.e., *Chew et al*., 2008]. Whereas the arc and back-arc regions have been largely studied in South America, little is known on the fore-arc region's evolution through time. In SW Ecuador, the El Oro metamorphic province is considered to have been in a fore-arc position since Paleozoic times [*Noble et al*., 1997; *Riel et al*., 2013] and represents a unique opportunity to understand the behavior of fore-arc regions during active subduction throughout the Mesozoic. The El Oro metamorphic province is located in a key position, close to the Huancabamba deflection that separates the central Andes from the northern Andes (Figure 1). North of the deflection, the northern Andes (Ecuador and Colombia) strikes NNE and is built on multiple oceanic terrane accretion since Cretaceous time [*Jaillard et al*., 2009]. South of the deflection, the central Andes (Peru) strikes NW-NNW and does not present evidence of exotic terrane accretion.

One of the major questions concerns the E-W subvertical orientation of the structures of the El Oro metamorphic province between the NNE striking northern Andes and the NW-NNW striking central Andes (Figure 2). Two models have been proposed in order to explain this orientation. *Aspden et al*. [1995] proposed that the subvertical structures of the El Oro metamorphic province were related to the development of a vertical high-temperature crustal shear zone during Triassic times, associated with the emplacement of the Piedras gabbroic pluton in its core (Figure 3a). *Gabriele* [2002] relates the E-W subvertical structures to the tilting of the Tahuín Group after the tectonic underplating of the gabbro and blueschist units, during a Late Triassic extensional event (Figure 3b) with a final, compressional stage of exhumation during Cretaceous times. The aim of our study is to better understand the geological events, which led to the juxtaposition of this

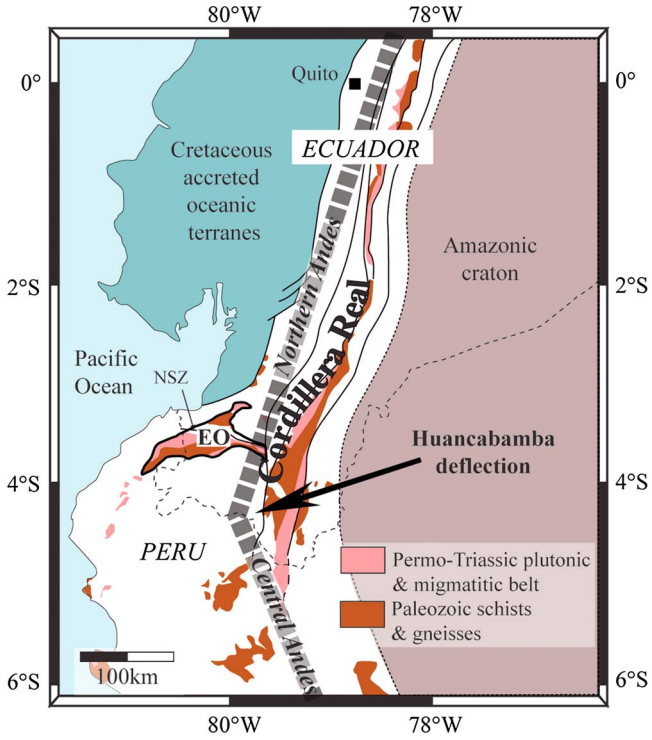

Figure 1. Simplified geological map of Ecuador and northern Peru modified after *Chew et al.* [2007] with the location of the El Oro metamorphic province. EO: El Oro and NSZ: Naranjo shear zone.

composite massif throughout the Mesozoic. In order to constrain this evolution, we have combined structural data, thermal modeling, and available geochronological data. This study provides new contrains on the connection zone between the northern and central Andes (Huancabamba deflection) during Mesozoic times, showing that the evolution of the El Oro metamorphic province until the Cretaceous was controlled by active subduction (central Andean tectonic style) while the evolution of the El Oro metamorphic province until the Cretaceous was controlled by the accretion of the oceanic terranes against the northern Andean margin.

2. Geological Overview of the El Oro Massif

The El Oro massif or metamorphic province comprises both continental units and terranes of oceanic affinity [*Feininger*, 1978], assembled in a fore-arc position since Paleozoic times [*Noble et al.*, 1997; *Riel et al.*, 2013]. To the north, the Jubones fault zone separates the El Oro metamorphic province from oceanic terranes accreted in the Late Cretaceous-Paleogene and overlying tertiary volcanic deposits; to the east, the El Oro metamorphic province is separated from the metamorphic rocks of the Cordillera Real by the Guayabal fault zone; and to the south, it is unconformably overlain by the volcano-sedimentary deposits of the Cretaceous Celica-Lancones basin (Figure 2). Following the terminology of *Gabriele* [2002], the El Oro metamorphic province can be subdivided into three main geological juxtaposed complexes: from north to south, the Birón Complex, the Raspas Complex, and the El Oro Complex (Figure 4).

2.1. Birón Complex

The Birón Complex constitutes the continental basement exposed north of the Raspas Complex (Figure 2). This complex is mainly composed of metapelitic and metapsammitic rocks to the north and of granitoids, migmatites, and amphibolites to the south. The main metamorphic foliation strikes E-W and is subvertical. Within the migmatites, several generations of leucosomes suggest multiple events of migmatization [*Gabriele*, 2002]. Our observations show that from north to south, the metamorphic grade progressively increases from andalusite-bearing metapelite to metatexite migmatites and diatexite migmatites containing plutonic bodies. U-Pb geochronology on monazite yielded two groups of ages at 200 ± 30 Ma and ~60–70 Ma [*Noble et al.*, 1997] for a granitoid. A major body of amphibolitized metagabbroic pluton striking E-W is dated at 75 ± 0.5 Ma by the Ar/Ar method on hornblende [*Gabriele*, 2002] and at 73.6 ± 0.5 Ma by the U-Pb method on zircon [*Riel*, 2012]. The ages at 60–70 Ma are interpreted as the result of an episode of intense deformation at high temperature during accretion of the Pallatanga oceanic terrane to the north, while the age of 200 ± 30 Ma is related to the Late Triassic metamorphic event recorded in the El Oro Complex [*Noble et al.*, 1997].

2.2. La Palma Shear Zone

To the south, the La Palma shear zone (Figures 2 and 4) separates the Birón Complex from the Raspas Complex. The shear zone is 10–50 m wide and is characterized by mylonitized quartz-rich micaschists with mafic and ultramafic eclogite and various metapelite boudins retrogressed under greenschist facies [*Gabriele*, 2002]. In the *x-z* plane of the finite strain ellipsoid, sigmoid-like ultramafic boudins show dextral movement. Ar/Ar dating on

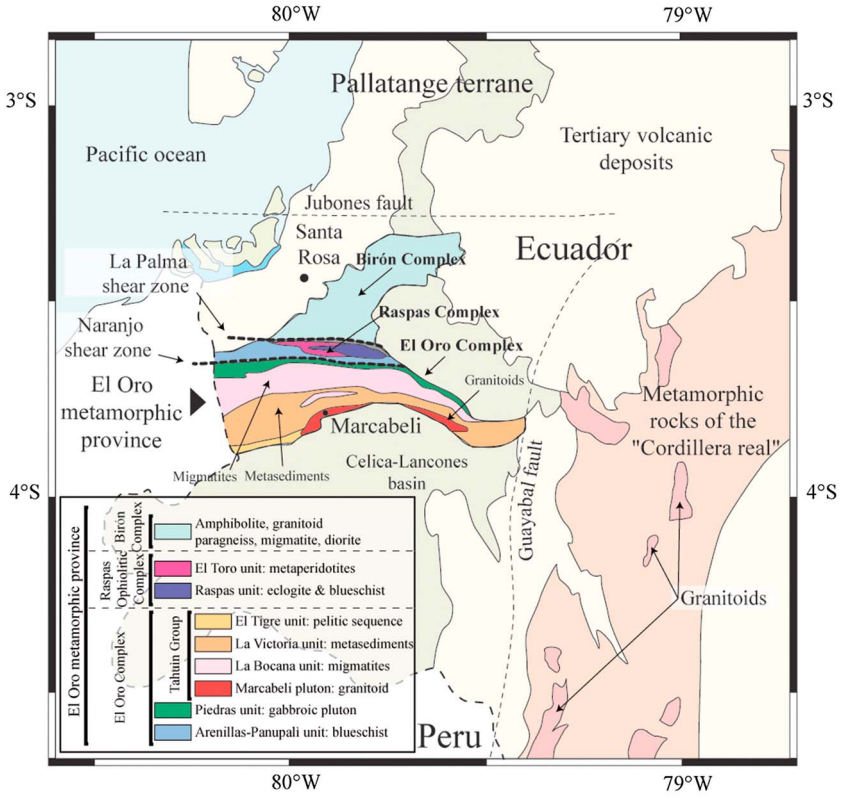

Figure 2. Simplified geological map of southwest Ecuador.

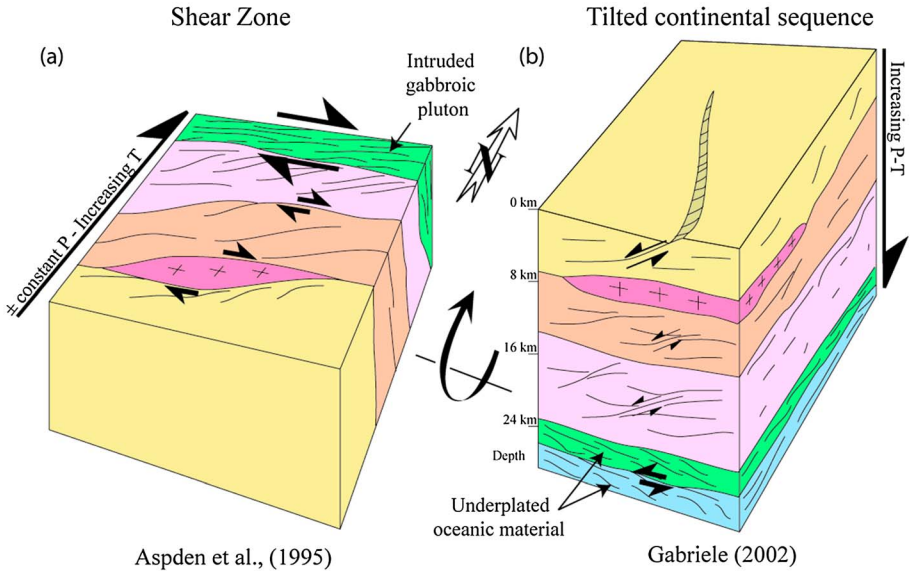

Figure 3. Schematic 3-D diagrams of the El Oro metamorphic province during Late Triassic times. (a) Dextral shear zone model of *Aspden et al*. [1995]. In this model, emplacement of the gabbroic Piedras unit in a vertical crustal shear zone triggered partial melting and emplacement of the Marcabeli and El Prado granitoid plutons. (b) Model of continental sequence partially molten during Late Triassic times [*Gabriele*, 2002]. In this model, the Piedras and the Arenillas-Panupalí units represent two distinct episodes of oceanic underplating, and the whole section was tilted during Late Triassic times. Same color chart as for Figure 2.

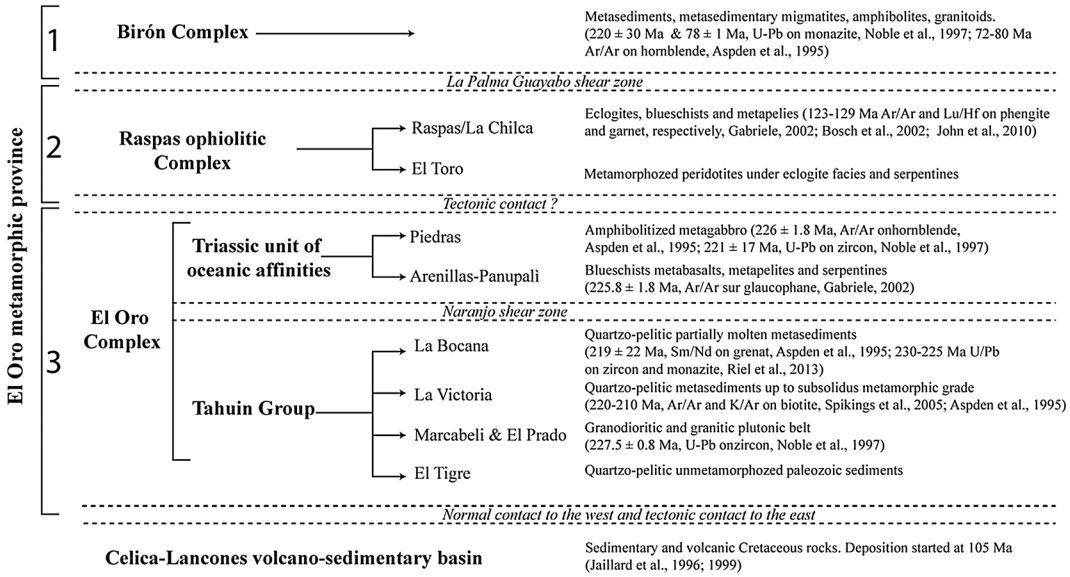

Figure 4. Nomenclature of the lithological complexes, groups, and units forming the El Oro metamorphic province. Lithologies and metamorphic ages of each unit are indicated on the right part of the diagram.

muscovite yielded an integrated age of 129.5 ± 0.9 Ma with a younger step at ~65 Ma [*Gabriele*, 2002], suggesting two distinct tectonic events.

2.3. Raspas Complex

The Raspas Complex is an ophiolitic succession metamorphosed under blueschist and eclogite facies conditions during Early Cretaceous times [*Gabriele*, 2002; *Gabriele et al.*, 2003; *John et al.*, 2010]. This complex comprises the metaperidotitic unit of El Toro and the high pressure (HP) rocks of the Raspas unit (Figure 5). The main foliation (defined by garnet + omphacite + phengite mineral assemblage) developed within the Raspas

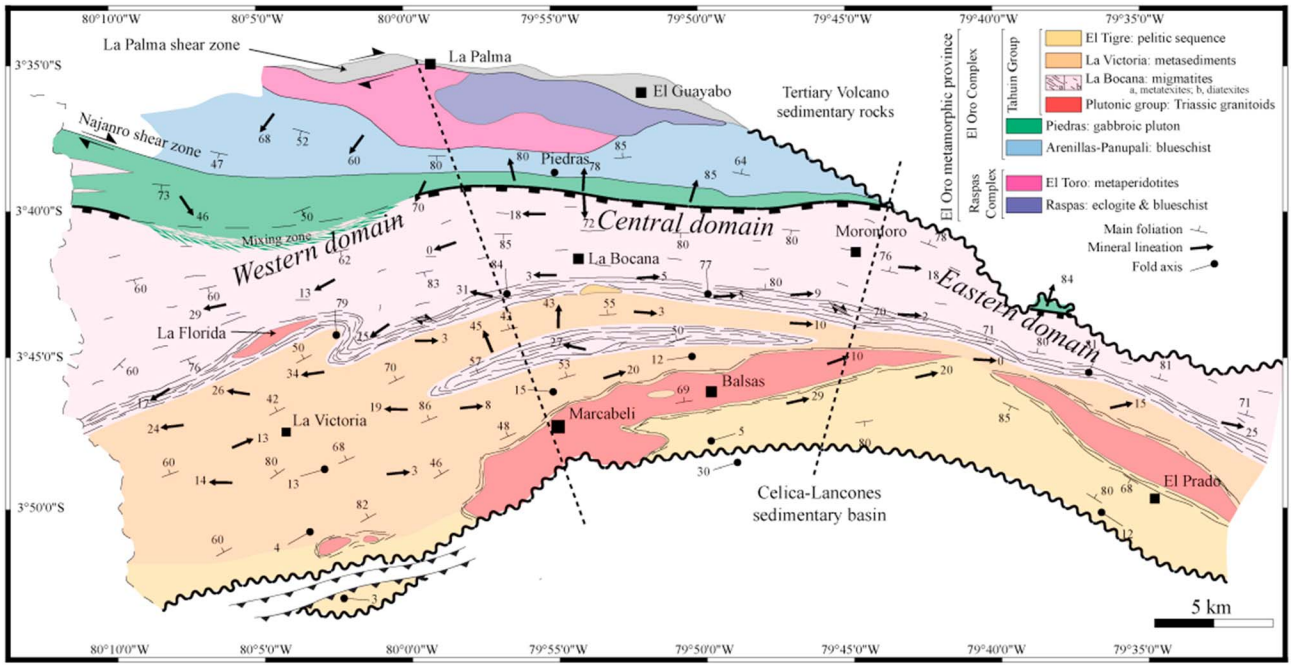

Figure 5. Geological and structural map of the El Oro metamorphic province. The continental basement exposed in the Birón Complex has not been represented. In the western part, the contact between the La Bocana and Piedras units corresponds to a primary, mixing magmatic contact between these units. The heavy black dashed lines indicate the boundary between western, central, and eastern parts of the El Oro metamorphic province.

Complex strikes E-W with a variable dip ranging from 60° to 90° toward the north. The main eclogitic foliation is folded by a secondary phase of deformation showing a vertical schistosity striking NE-SW to E-W [*Gabriele*, 2002]. The blueschist unit exhibits seamount geochemical signatures, while the eclogites have a mid-ocean ridge basalt (MORB) affinity [*John et al*., 2010]. Peak metamorphic conditions in the eclogites have been estimated at 600 ± 50°C and 18 ± 2 kbar, and the age of the HP metamorphism has been constrained by Lu-Hf dating on garnet at ~130 Ma [*John et al*., 2010]. Thermochronological ages of the eclogite-facies rocks on phengite at 129–123 Ma [*Gabriele*, 2002] show that cooling occurred shortly after the HP metamorphism.

2.4. The El Oro Complex

South of the Raspas Complex and separated by a hidden contact, the El Oro Complex is made up of terranes of continental and oceanic affinities juxtaposed during Late Triassic times [*Gabriele*, 2002; *Riel et al*., 2013]. From north to south, the El Oro Complex is made of the blueschists of the Arenillas-Panupalí unit, the amphibolitized metagabbro of the Piedras unit, and the continental sequence of the Tahuín Group. The metamorphic conditions, geochemistry, and ages of this complex are relatively well constrained; however, little is known on its internal structures and the geological event that led to the amalgamation of this complex.

2.4.1. Arenillas-Panupalí Unit

The northernmost Arenillas-Panupalí unit constitutes a 1 to 4 km thick blueschist unit comprising predominantly blueschist facies metabasalts (Figure 6h) and metasediments, with minor serpentinites. In the metabasalts, the peak metamorphism is recorded by the assemblage garnet + glaucophane + titanite and retrogression in greenschist facies by albite + chlorite + epidote [*Gabriele*, 2002]. The peak pressure-temperature (P-T) estimates on the metabasalt are of ~9 kbar and ~300°C [*Gabriele*, 2002]. The main foliation strikes E-W and dips at a high angle (60–90°) to the south. *Bosch et al*. [2002] showed that the metabasalts have MORB-like geochemical signatures. Formerly considered to be Cretaceous in age on the basis of its blueschist metamorphic conditions [*Aspden et al*., 1995], Ar/Ar datings on amphiboles from the Arenillas-Panupalí unit yielded ages of 225.2 ± 2.7 and 226 ± 1.8 Ma [*Gabriele*, 2002]. The Arenillas-Panupalí unit is in a key position as it separates the Cretaceous Raspas Complex to the north from the Triassic Piedras gabbroic unit to the south. Unfortunately, the northern contact zone could not be observed due to pervasive equatorial weathering and dense vegetation cover.

2.4.2. Piedras Unit

The gabbroic Piedras unit is separated from the Arenillas-Panupalí unit by the amphibolite facies dextral Naranjo shear zone. The Piedras unit is made of E-W striking, saussuritized and amphibolitized metagabbro (Figure 6g), with a few ultramafic bodies. The metagabbro has MORB-like geochemical signatures [*Aspden et al*., 1995; *Gabriele*, 2002], and U-Pb dating on zircon yielded a magmatic age of 221 ± 17 Ma [*Noble et al*., 1997]. An Ar/Ar age on amphibole constrains the age of cooling through ~550°C at 226 ± 2.1 Ma [*Gabriele*, 2002]. Based on evidence of mixing between basic and felsic magma in its southwestern contact with the Tahuín Group, the Piedras unit has been interpreted as an underplated magmatic body [*Aspden et al*., 1995; *Riel et al*., 2013].

2.4.3. Tahuín Group

Separated from the Piedras unit by a greenschist facies mylonitic shear zone [*Aspden et al*., 1995; *Gabriele*, 2002], the Tahuín Group corresponds to the continental basement exposed south of the Piedras unit [*Feininger*, 1978; *Gabriele*, 2002; *Riel et al*., 2013]. This continental sequence is composed from south to north by Devonian sediments [*Martínez*, 1970] of the El Tigre unit (Figure 6a), Late Triassic granitoids of the Marcabeli and the El Prado plutons [227.5 ± 0.8 Ma with U-Pb method on monazite, *Noble et al*., 1997] (Figure 6b), metasediments of the La Victoria unit characterized by a northward increasing metamorphic grade [*Feininger*, 1978] (Figure 6c), and by the Late Triassic migmatitic complex of the La Bocana unit (Figure 5 and Figures 6d–6f). On the scale of the massif, the main foliation roughly strikes E-W and dips steeply. P-T conditions in the La Bocana unit evolve from 4–5 ± 2 kbar and 650 ± 50°C in the south to 5–8 ± 2 kbar and 720–800 ± 50°C in the north [*Riel et al*., 2013]. High-temperature metamorphism and *S*-type magmatism in the Tahuín Group have been dated by various methods and show a well-defined Late Triassic crystallization age at 230–225 Ma [*Aspden et al*., 1995; *Noble et al*., 1997; *Spikings et al*., 2005; *Riel et al*., 2013] (Figure 7). Mineral cooling ages determined by the Ar/Ar and K/Ar methods on biotite are slightly younger and range from 220 to 210 Ma [*Spikings et al*., 2005].

3. Structural Analysis in the El Oro Complex

Our field mapping has allowed us to recognize four successive deformation events (referred to as D_1 to D_4; Figure 8), which can be distinguished on the basis of the geometry, kinematics, and structural styles of the relevant

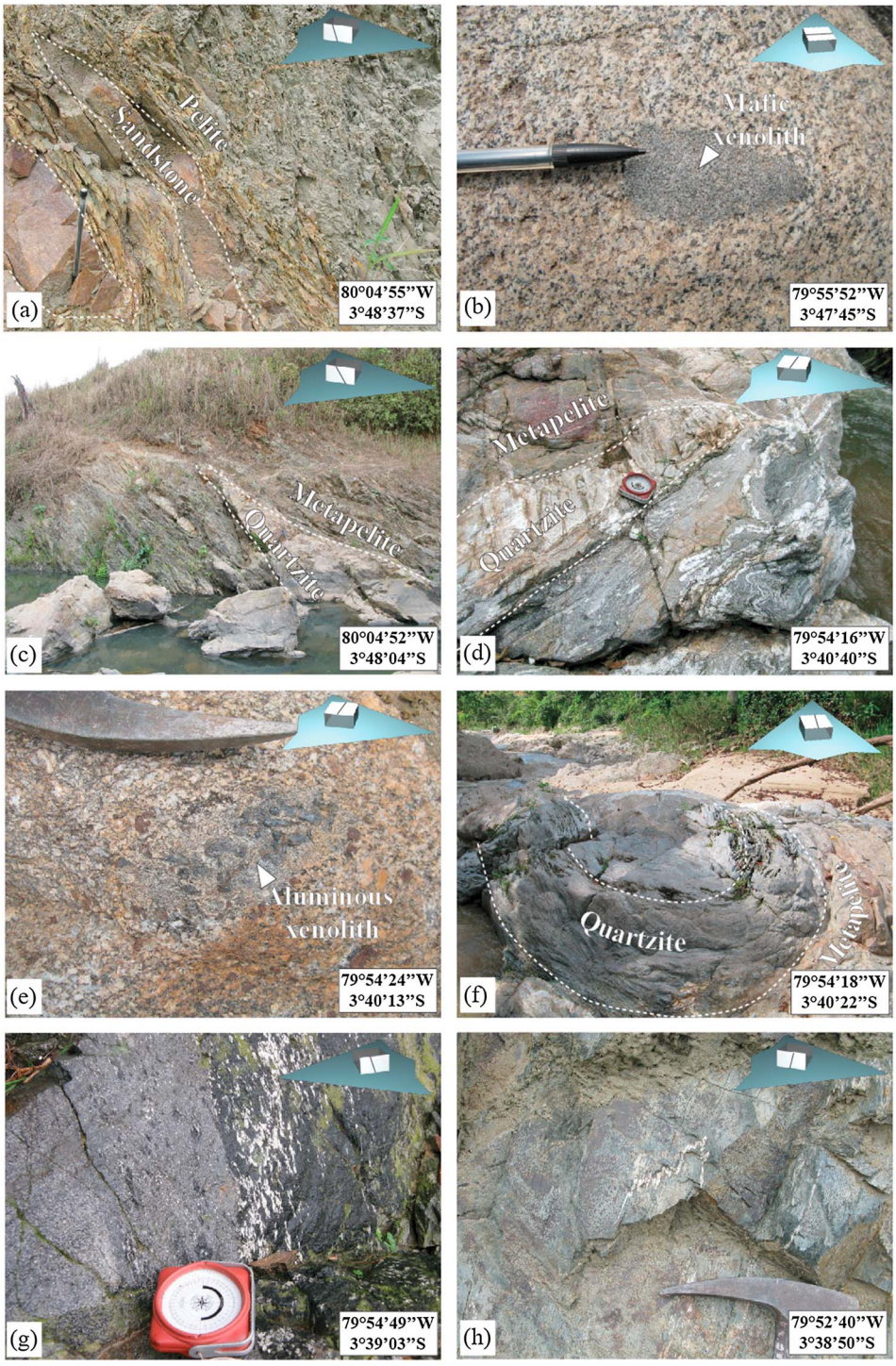

Figure 6. Photographs of representative lithologies of the El Oro metamorphic province. (a) Pelite/psammite succession of the El Tigre unit. (b) Mafic xenolith in a granodiorite lithology of the Marcabeli pluton. (c) Metapelite/quartzite alternation in the La Victoria unit. (d) Metapelite/quartzite alternation in the upper part of the La Bocana unit; metapelitic layers are partially molten and exhibit folded leucosomes while quartzitic boudinaged layers show tensile fractures. (e) Garnet-bearing diatexite mesocratic migmatite of the lower La Bocana unit; note the presence of a partially molten sillimanite-rich metasedimentary xenolith. (f) High-temperature fold related to D_1 deformation and marked by quartzite layers, a few kilometers south of the La Bocana locality. (g) Typical magmatic texture on the Piedras metagabbroic unit. (h) Metabasalt in blueschist facies of the Arenillas-Panupalí unit. The blue arrows represent the north direction lying in a horizontal plane, the highlighted face of the cube shows the observed plane surface of the outcrop compared with the horizontal, and finally the line on the highlighted face of the cube shows the azimuth of the foliation (same as in Figures 10–13).

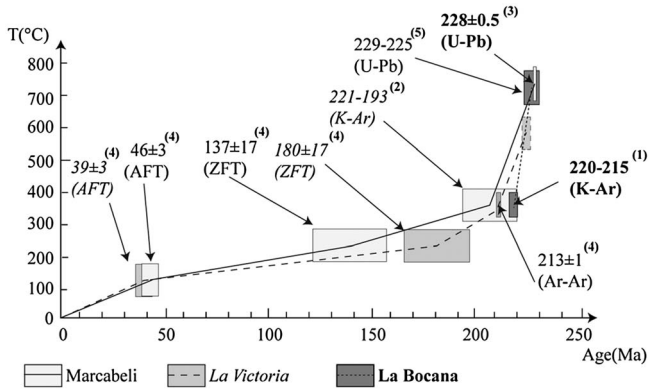

Figure 7. Cooling temperature (°C) versus age (Ma) of the Marcabeli, La Victoria, and La Bocana units of the Tahuín Group. Ages are reported from *Feininger and Silberman* [1982], *Aspden et al.* [1992, 1995], *Noble et al.* [1997], *Spikings et al.* [2005], and *Riel et al.* [2013]. K/Ar ages are on biotite, and U-Pb ages are on monazite and zircon.

structures, from mass scale to thin section made from oriented samples. The description of the metamorphic foliation and the stretching lineation allows us to constrain the finite strain pattern.

3.1. Early, Synmigmatitic Deformation (D_1)

The first deformation event (D_1) is associated with HT metamorphism in the Tahuín Group (from greenschist to granulite facies) and in the amphibolitized gabbros of the Piedras unit.

3.1.1. D_1 Deformation in the La Victoria Metasedimentary Unit

The D_1 deformation event could only be identified in the western and central domains of the massif, close to the migmatitic unit, where the D_4 stage of deformation was less intense. In the southwestern part of the La Victoria unit, D_1 is characterized by the development of the metamorphic S_1 foliation. The stretching and recrystallization of *K*-feldspar, replaced by sericite, marks the associated L_1 mineral lineation. In the northern part of the La Victoria unit, L_1 is marked by prismatic sillimanite. S_1 strikes SW-NE and dips to the NW in the

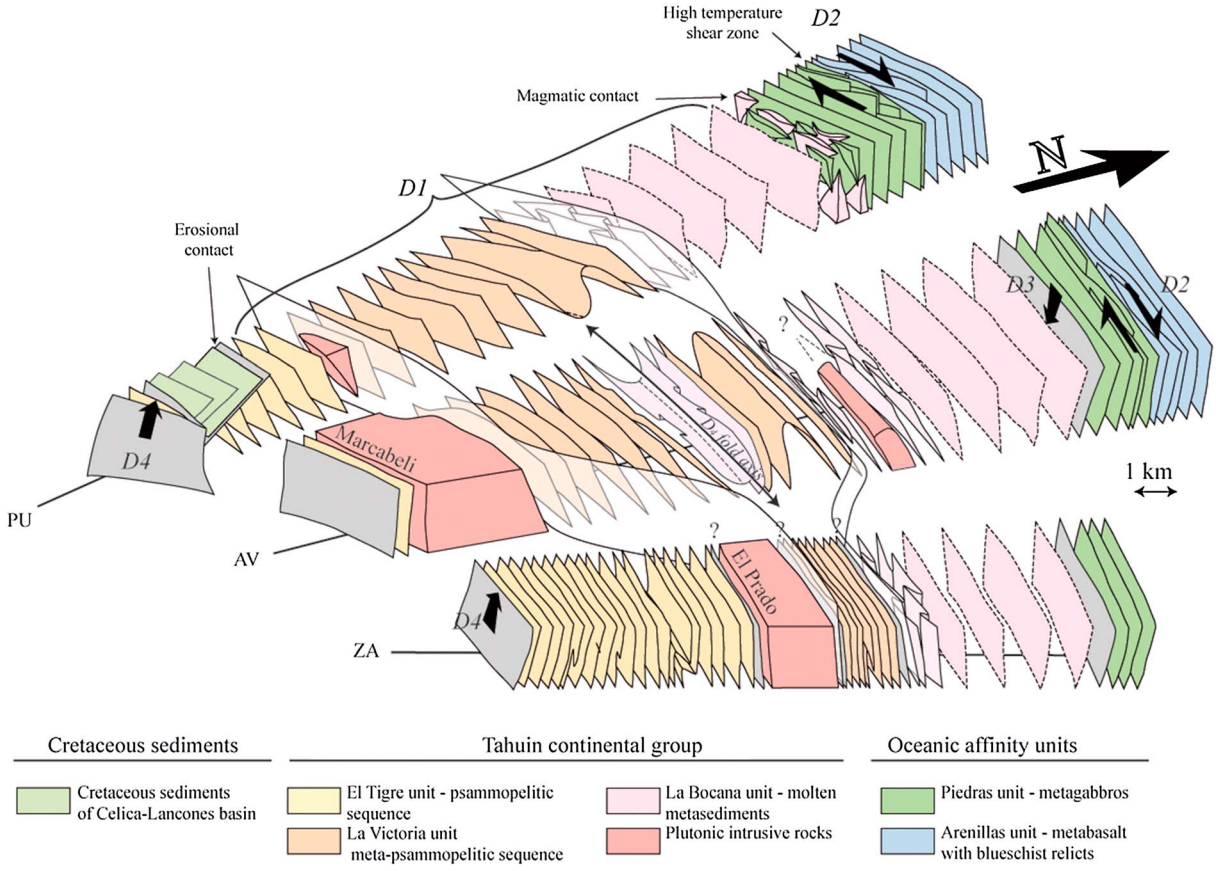

Figure 8. The 3-D schematic block diagram showing the present-day geometry of the El Oro province. In this diagram D_1 to D_4 stages of deformation are illustrated. Note that the thickness of the La Victoria unit is highly reduced toward the east, while the thickness of the La Bocana unit remains more or less constant. Note that the transparent planes outlined in heavy black show the boundaries of the La Victoria unit and that AV, PU, and ZA correspond to the acronym for the three studied cross sections: La Avanzada, Puyango, and Zaruma, respectively.

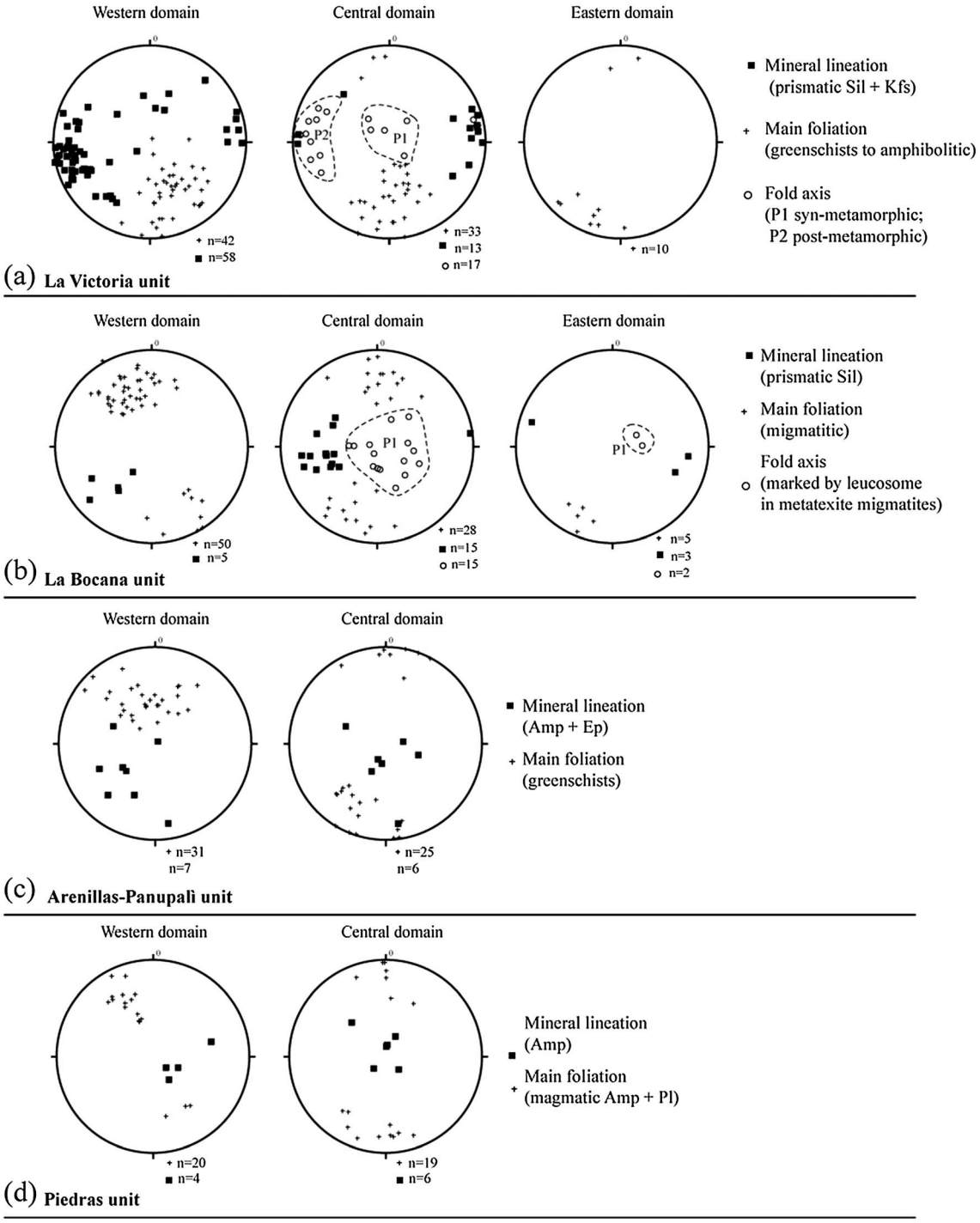

Figure 9. Stereonets (lower hemisphere, equal area) of planar and linear elements of the El Oro Complex. (a) La Victoria unit. (b) La Bocana unit. (c) Arenillas-Panupalí unit. (d) Piedras unit.

western domain, strikes E-W and dips to the north (20 to 60°) in the central domain, and strikes WNW-ESE with a subvertical dip in the eastern domain of the massif (Figure 9a). L_1 generally gently plunges to the WSW in the western domain and E in the central domain (Figure 9a).

In this section, in the *x-z* plane, several shear criteria such as sigma-type *K*-feldspar porphyroblasts, muscovite porphyroblasts (Figure 10a), and syntectonic andalusite porphyroblasts intergrown with sillimanite (Figure 10b) show internal surface deflected by a dextral shear.

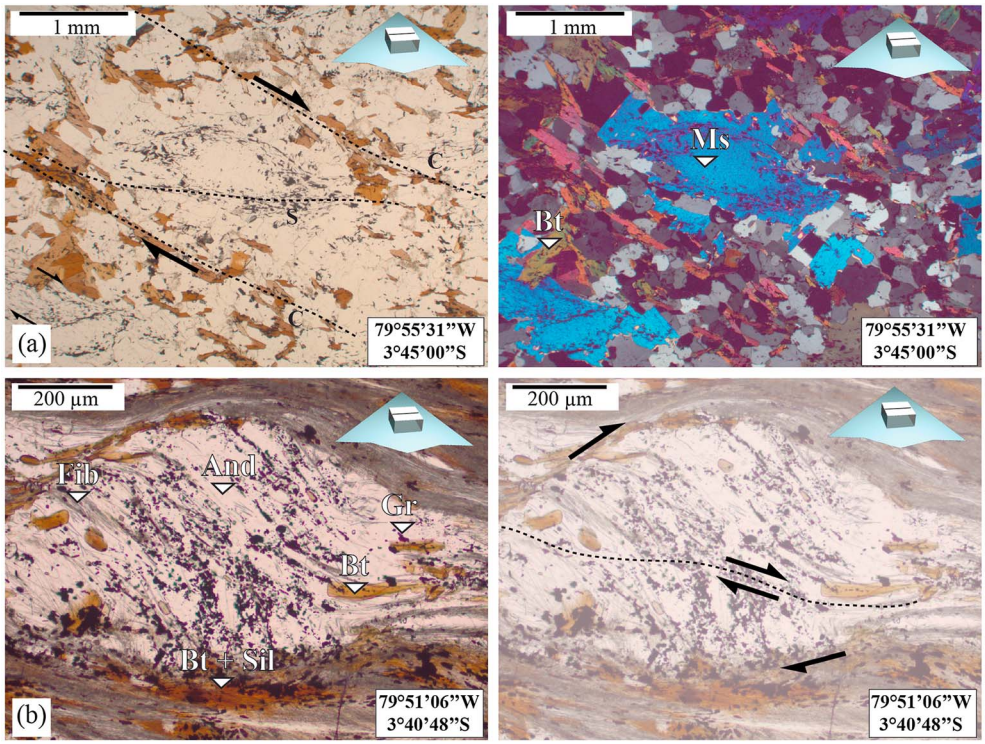

Figure 10. Microphotographs of the D_1 deformation event in the La Victoria unit. (a) Late recrystallization of muscovite crosscutting the main foliation. Graphite inclusions in the muscovite exhibit a dextral sigmoid-like sense of shear. Note that the former crystal was likely surrounded by these inclusions and that recrystallization occurred with *K*-rich fluid influx. (b) Syntectonic growth and recrystallization of andalusite porphyroblasts into fibrolite. In the *x-z* plane, the andalusite crystal shows a 50–55° clockwise rotation marked by graphite, fibrolite, and biotite inclusions. Moreover, a dextral shear band is evidenced in the andalusite crystal. The fact that the fibers of sillimanite are rotated together with the andalusite crystal indicates intergrowths of both minerals, thus constraining the P-T conditions of the syntectonic growth along the reaction curve between andalusite and sillimanite (450 to 650°C for 4.3 to 2.8 kbar). Blue arrows: same as in Figure 6.

3.1.2. D_1 Deformation in the La Bocana Migmatitic Unit

In the La Bocana unit, the S_1 synmigmatitic foliation strikes WSW-ENE and steeply dips to the SE in the western domain (Figure 9b). In the central domain, S_1 strikes W-E and strongly dips to the south and to the north in the upper and lower units, respectively. In the eastern domain, S_1 strikes NW-SE and steeply dips to the NE. Associated L_1 lineation is marked by prismatic sillimanite, which dips at low angle and shows the same change in strike from NW-SE dominantly plunging to the west, to E-W, plunging to the east.

The upper (southern) migmatitic part of the La Bocana unit (Figure 5) constitutes an ~2 km thick layer composed of metatexite with a northward increasing proportion of leucosome from few percent up to 50%. The characteristic mineral assemblage is quartz + biotite + fibrolite + *K*-feldspar + plagioclase ± prismatic sillimanite. In this unit, quartzitic competent layers are unmolten and fractured by fluid pressure increase due to southward percolating anatectic melts via dilatant structures (Figure 11b), while metapelitic incompetent layers with leucosome are sheared and folded. South of the locality of La Bocana, asymmetric folds in metatexite migmatite exhibit subvertical axes with geometry compatible with dextral sense of shear (Figure 11b). Few kilometers east of the La Bocana locality, at the transition zone between the upper and the lower migmatitic units, shear zone associated with folds also indicates dextral transpressive shearing (Figure 11c).

The lower (northern) migmatitic part of the La Bocana unit (Figure 5) is ~8 km thick and essentially composed of metasedimentary mesocrate diatexites. The dominant paragenesis is quartz + garnet + biotite + plagioclase + prismatic sillimanite, and the foliation is marked by schlieren of biotite + sillimanite. In the *x-z* plane, deformation is marked by elongated xenoliths of metasedimentary origin exhibiting an E-W trending orientation (Figures 6e and 11d). A few kilometers north of the La Bocana locality, a decametric fold marked

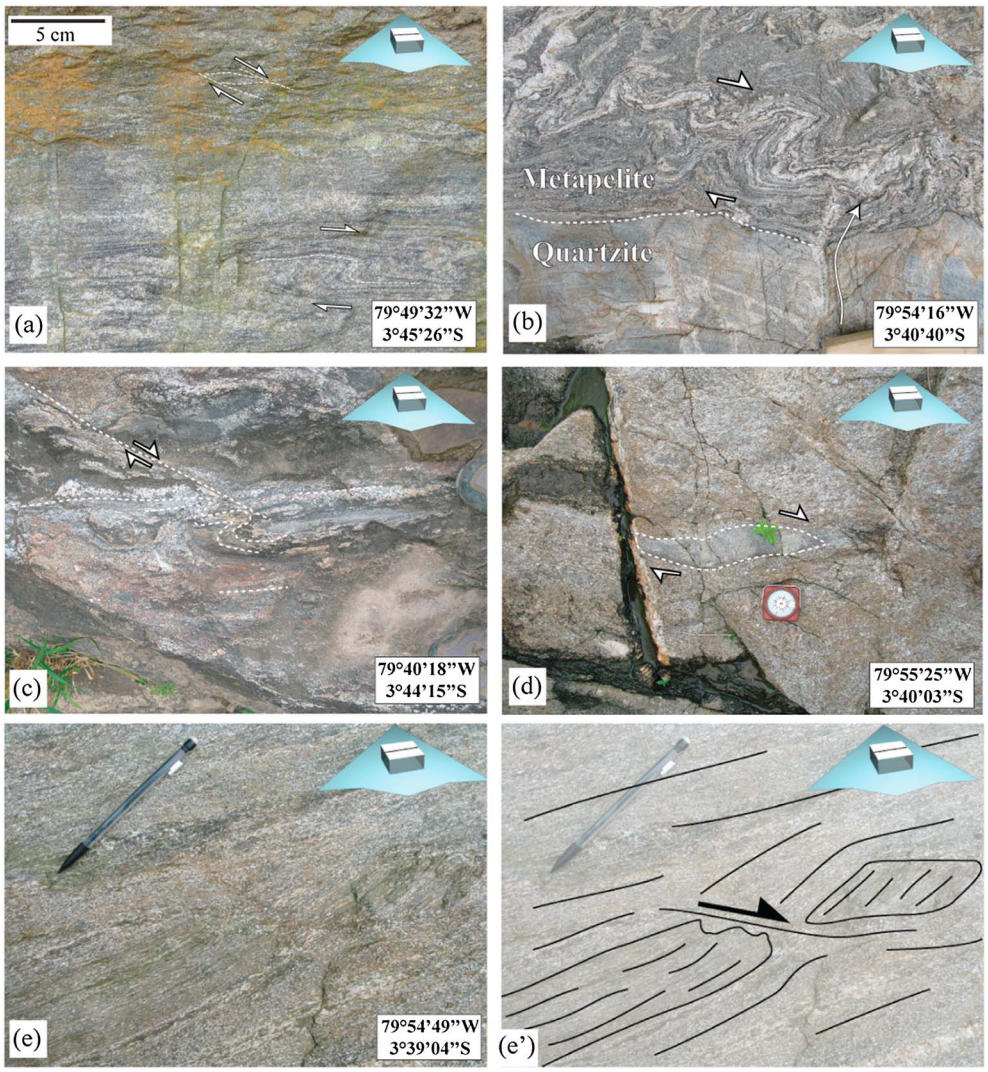

Figure 11. Field-scale photographs of the D_1 deformation-related structures. (a) Photograph of a migmatitic contact at the northern boundary of the Marcabeli granitoid. In the *x-z* plane, folded leucosome and melanosome and CS structures show a synmetamorphic dextral sense of shear indicating syntectonic dextral emplacement of the Marcabeli granitoid. (b) Photograph of partially molten layers in the upper La Bocana unit in the *x-z* plane. The photograph shows heterogeneous strain pattern between undeformed quartzitic layers and partially molten metapelitic layers with a dextral sense of shear marked by leucosome layers. The white arrow shows the magma pathway direction through the quartzitic layer. (c) Dextral transpressive ductile shear zone at the top of the lower La Bocana unit in the *x-z* plane. The southern block exhibits centimetric folding compatible with a dextral transpressive sense of shear. (d) Sheared quartzitic xenolith in garnet-bearing mesocrate diatexite of the lower La Bocana unit. Either simple or pure shear can explain the structure depending on the primary orientation of the xenolith with respect to the main stress direction. (e) Magmatic foliation in the Piedras gabbroic unit. Melagabbro layer within leucogabbro layers are disrupted and show a dextral sense of shear. Blue arrows: same as in Figure 6.

by a quartzite body shows a subhorizontal, N-S trending axis (Figure 6f). We relate this geometry to complex folding within a melt-rich diatexite with a magma-like behavior.

3.1.3. D_1 Deformation in the Marcabeli and El Prado Plutons

In the western and central parts of the massif, the *S*-type granodioritic to granitic plutons of Marcabeli and El Prado [*Aspden et al.*, 1995] appear undeformed with numerous E-W oriented mafic xenoliths (Figure 6b). The xenoliths are generally rounded, medium to fine grained and have an amphibole-rich granodioritic composition. Partial melting in the metasediments near the contact with the pluton can be observed in a 10 to 50 m wide aureole. A few kilometers NW of Balsas (Figure 5), contact migmatite of metapelitic origin exhibit *C-S* structures and folded melanocrate/leucocrate layers. In the *x-z* plane, these kinematic indicators

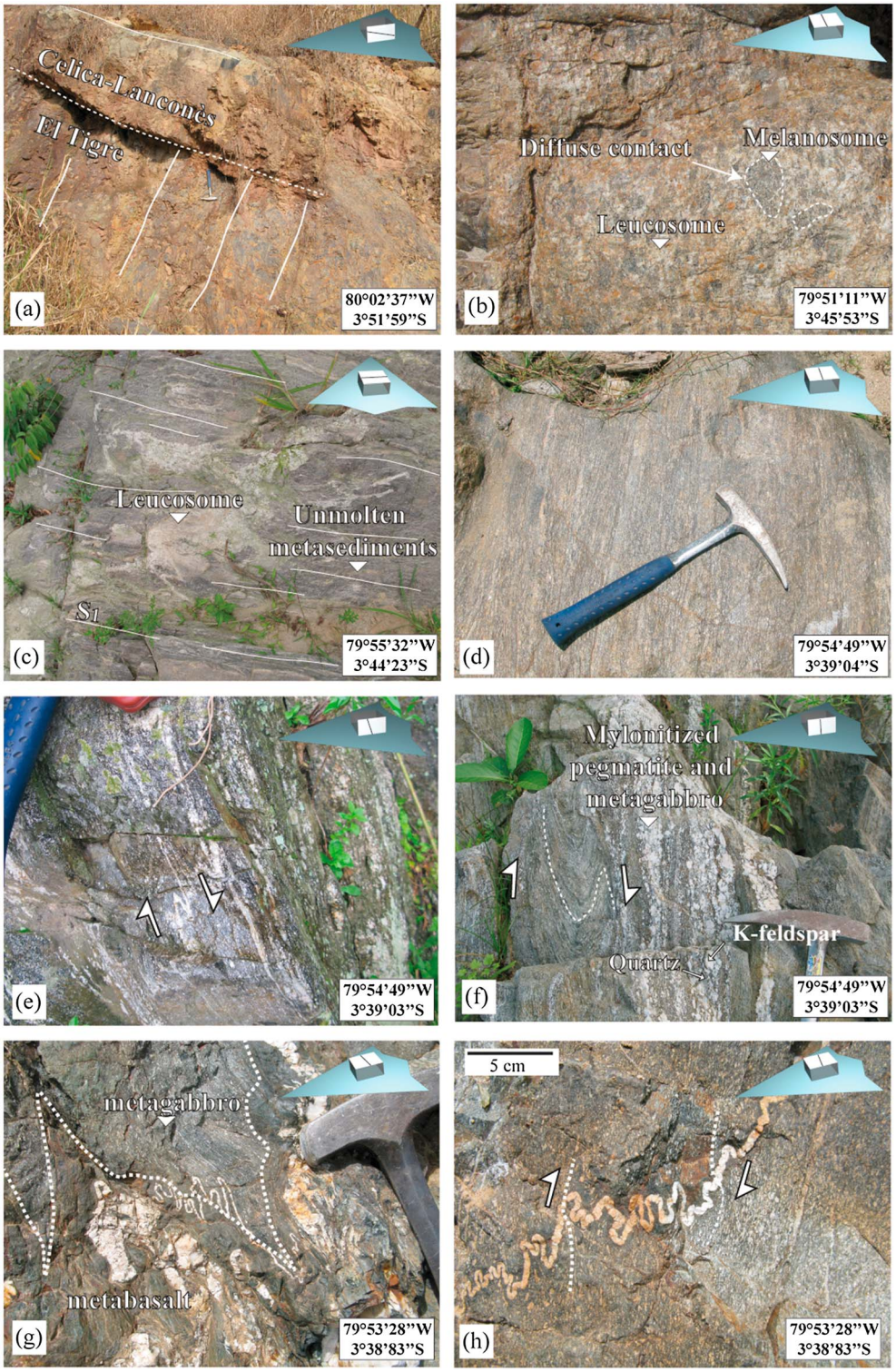

Figure 12

are consistent with a dextral sense of shear (Figure 11a). Between the Balsas and Marcabeli localities, within the Marcabeli granitoid, a 100 m large lense of metasediment shows evidence of partial melting. In this contact migmatite, centimetric patches of biotite-rich melanosome and leucosome have diffuse contacts and do not exhibit any preferred orientation (Figure 12b); they are compatible with dominant flattening. Strain partitioning with a combination of coaxial flattening and noncoaxial shear criteria is widespread and coherent with a transpressive regime.

3.1.4. D_1 Deformation in the Piedras Gabbroic Unit

North of the La Bocana unit and separated by the Naranjo shear zone, the Piedras unit is composed of amphibolitized gabbro (Figure 6g). The Piedras gabbroic unit exhibits magmatic textures with layering of millimetric-grained leucogabbro and centimetric-grained melagabbro (Figure 6g). The mean foliation S_1 strikes WSW-ENE; it dips steeply to the SSE in the western domain (Figure 9d), while it strikes E-W and is subvertical in the central domain. The mineral lineation L_1, which is marked by a preferred orientation of amphiboles, exhibits a consistent subvertical trend (Figure 9d) and is interpreted as a stretching lineation. In some places, evidence of melagabbro crystallizing before leucogabbro is marked by sheared and disrupted layers of melagabbro, showing a dextral sense of shear (Figure 11e).

3.2. Synpeak to Postpeak Metamorphic Event (D_2)

The early event D_2 finite strain pattern is restricted to the contact zone between the oceanic, Arenillas-Panupalí basaltic unit, and the Piedras gabbroic unit (the Naranjo shear zone). Within a 100 to 200 m wide area, the contact zone is folded by millimeter to decimeter-scale asymmetric isoclinal folds. North of the Piedras locality, the contact between the metabasalts of the Arenillas-Panupalí blueschists and the gabbro of the Piedras unit is cut by the main foliation. This crosscutting is associated with the intrafoliar development of plagioclase veins (Figure 12g). The shear criteria marked by intrafoliar folds of plagioclase veins with subvertical axis are consistent with a dextral transpressive sense of movement (Figure 12h). The L_2 lineation is marked by the orientation of amphibole and plagioclase in the gabbroic lithology and is subhorizontal with an E-W trend. On the northern side of the shear zone, the metabasalt lithology related to the Arenillas-Panupalí unit is amphibolitized, and relicts of HP metamorphism are entirely erased.

3.3. Postmetamorphic Deformation (D_3)

Tertiary and quaternary volcano sedimentary deposits almost completely cover the tectonic boundaries of the El Oro metamorphic province limiting direct observations of the D_3 event. South of the Piedras locality, the contact zone between the La Bocana and Piedras units is made of a 20 m thick zone of mylonitized gabbro and garnet-bearing diatexite (Figure 12f) and minor mylonitized pegmatitic dykes. In the metagabbro, shear sense indicators marked by folded centimetric plagioclase layer and by folded melagabbro layer exhibit top-to-the-south normal movement (Figures 12e and 12f). At a macroscopic scale, mylonitized pegmatitic dykes together with the metagabbro exhibit centimetric angular and fractured porphyroblasts of plagioclase, while millimetric plagioclase are rounded and elongated along the direction of shear (Figure 12f). In the lower migmatitic unit, close to the tectonic contact, the migmatites are strongly mylonitized on a 10 m thick zone consistent with a strong N-S flattening component (Figure 12d).

Figure 12. Field photographs of the contact zone between the units of the El Oro metamorphic province south of the Raspas Complex. (a) Discordant contact between the Paleozoic sediment of the El Tigre unit and the Cretaceous sediments of the Celica-Lancones basin; note the angular unconformity of ≈90° between both units. (b) Partially molten metasedimentary xenolith in the northern part of the Marcabeli granodiorite. Note that the overall xenoliths size is 50 m long for 10 m large and is made of quartzite and partially molten metapelites. (c) Contact zone between the unmolten sediments of the La Victoria unit and the upper part of the La Bocana migmatites; leucosomes cross-cutting the foliation show the proximity of the partially molten zone. (d) The southern side of the contact zone between the Piedras and the lower La Bocana unit showing strongly mylonitized garnet-bearing migmatites. (e) Mylonitized metagabbro in the contact zone between the La Bocana and Piedras units in the central part of the studied area showing top-to-the-south normal sense of shear. (f) Mylonitized pegmatite dyke showing fracturing of centimetric plagioclase crystals. On the left side, folded melagabbro layer shows top-to-the-south normal shearing. (g) Contact zone between the gabbros of the Piedras unit and the metabasalt of the Arenillas-Panupalí unit. In the contact zone, the metabasalts are amphibolitized, showing that the emplacement of the blueschists occurred while the gabbro was still hot. (h) Dextral sense of shear underlined by a plagioclase vein within the metagabbro of the Piedras unit, close to the contact zone with the blueschists of the Arenillas-Panupalí unit. Blue arrows: same as Figure 6.

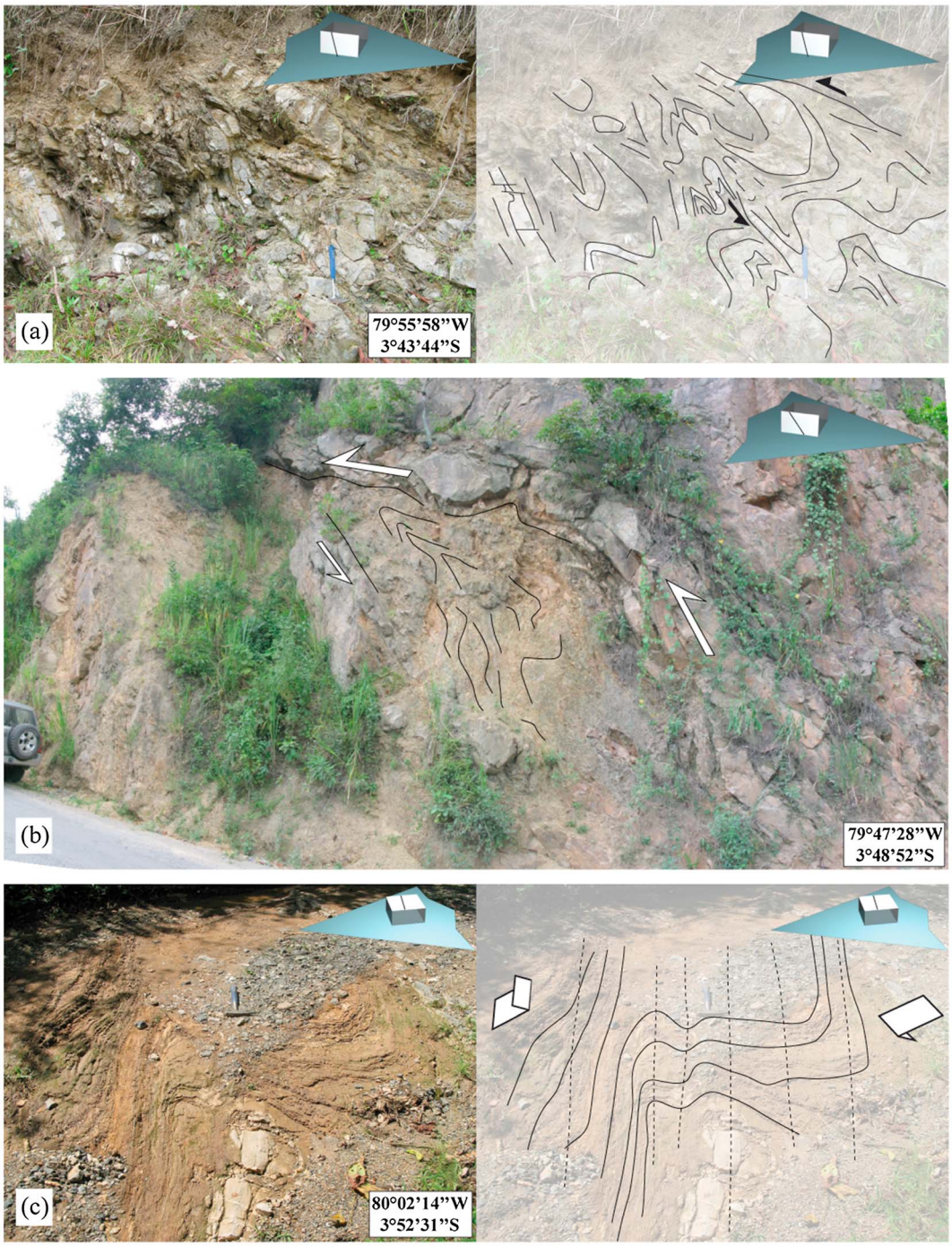

Figure 13. Field photographs of D_3-related deformation. (a) Asymmetric fold structures with south verging direction located south of the La Bocana locality. On the left, brittle fracturing shows south verging displacement. (b) South verging faulted fold in the El Tigre unit, in the eastern part of the massif. (c) South verging kink fold in the Cretaceous Celica-Lancones basin, south of the unconformable contact between the Paleozoic sediments of the El Tigre unit and the Cretaceous sediments of the Celica-Lancones basin, in the southwestern part of the massif. Blue arrows: same as Figure 6.

3.4. Upper Cretaceous Compressional Event (D_4)

Throughout the massif, the expression of D_4 deformation is heterogeneous and is predominantly expressed in the southern part of the El Oro Complex. With the exception of the eastern part of the El Oro Complex, where the Tahuín Group thickness is at a minimum, our observations show that the lower La Bocana unit, the Piedras unit, and the Arenillas-Panupalí unit are not, or weakly, affected by the D_4 event.

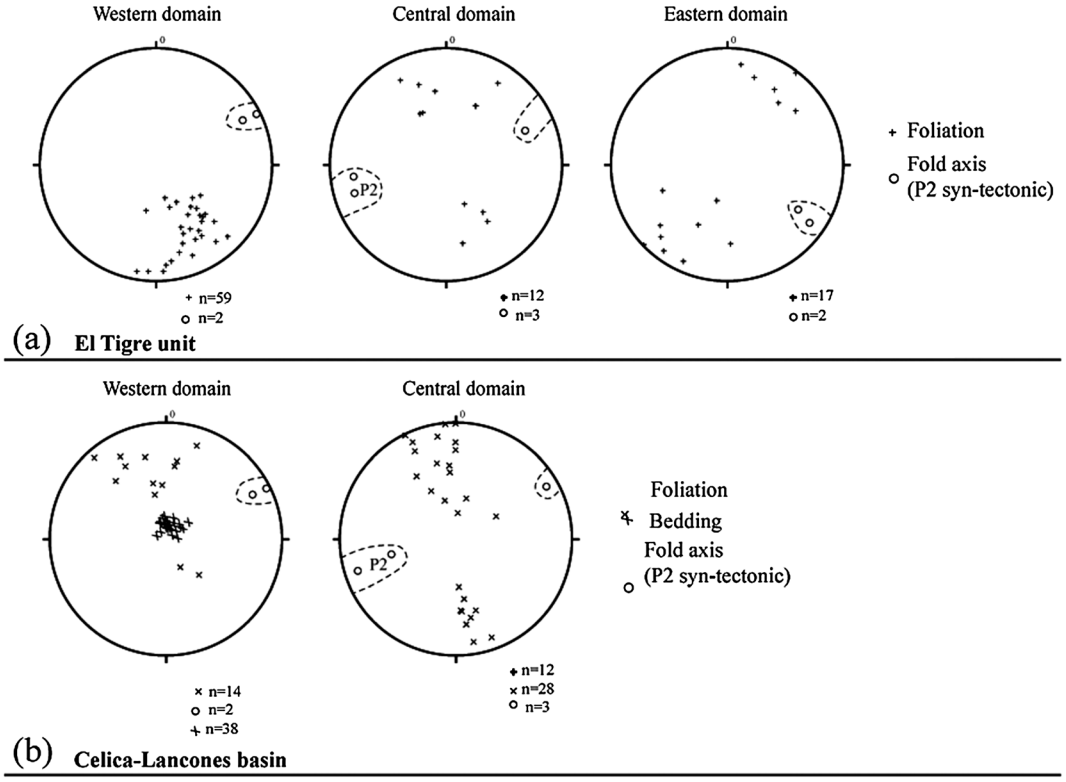

Figure 14. Stereonets of planar and linear elements of the El Oro Complex. (a) El Tigre unit. (b) Celica-Lancones basin. Note that bedding has been only reported for the Cretaceous sediments in the southwestern part of the massif.

4. D_4 Deformation in the Tahuín Group

In the central part of the Tahuín Group, this compressional phase is mainly represented by the fold marked by the appearance of the La Bocana unit within the La Victoria unit (Figure 8). This fold (interlimb angle 70–30°) has a present-day south verging axial plane with an E-W subhorizontal axis (Figures 5 and 8) [see also *Feininger*, 1978]. In the western part of the massif, folding of the metamorphic isograde indicates that D_4 is postmetamorphic peak (Figure 5). In the southwestern part of the massif, D_4 has not been observed and the sediments of the Celica-Lancones basin unconformably overlay the pelites of the El Tigre unit (Figure 12a). In the eastern part of the massif (Figures 4 and 5c), the regional D_4 folding is not observed, and the structures are strongly parallelized. In the central part of the La Victoria unit, D_4 is characterized by the development of south verging, asymmetric, subisoclinal folds with E-W subhorizontal axis (Figure 13a). In quartzitic layers, subhorizontal to weakly north dipping faults show southward displacement (Figure 13a). In the eastern part of the massif, in the El Tigre unit, D_4 is marked by southwest verging, asymmetric folds with E-W subhorizontal axis (Fgure 13b). In the easternmost part of the massif, south of the El Prado locality (Figure 5), the contact zone between the El Tigre unit and the sediments of the Celica-Lancones basin is faulted. The D_4 style of deformation in the contact zone is dominated by the development of a subvertical cleavage (S_4) developed in low grade metamorphic conditions.

5. D_4 Deformation in the Adjacent Celica-Lancones Basin

In the northeastern part of the Celica-Lancones basin (Figure 5), D_4 is characterized by a sheet of the Paleozoic El Tigre unit, thrust northward onto the Albian-Cenomanian sediments of the Celica-Lancones basin. The presence of metric, open to kink-like folds shows top-to-the-north sense of shear (Figure 13c). Associated lineations within quartzitic layer (L_4) trend N-S and plunge steeply to the south, thus indicating a top-to-the-north sense of shear.

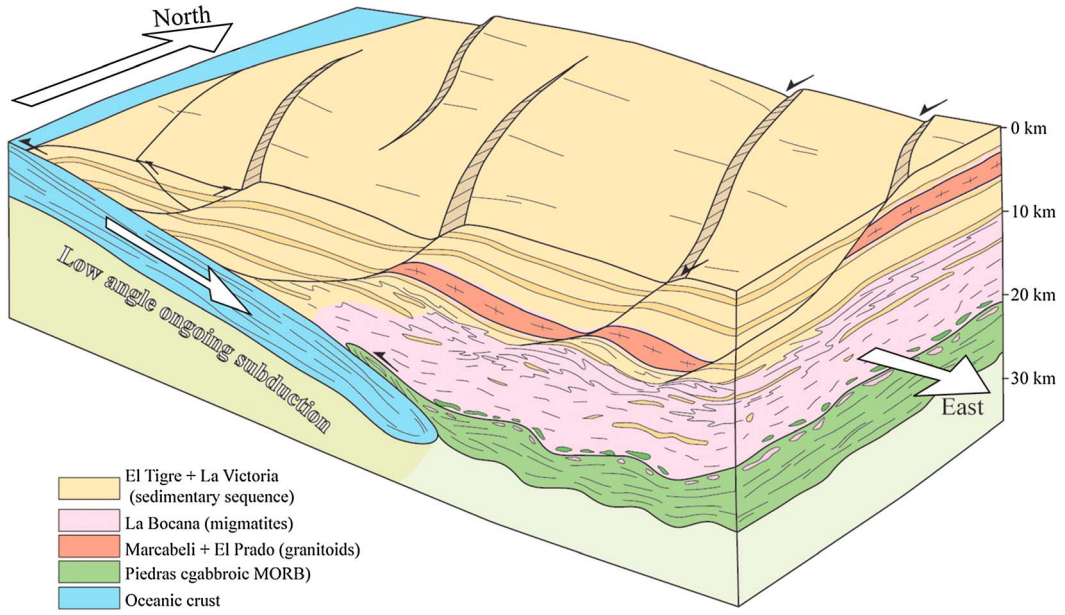

Figure 15. Schematic 3-D diagram of the El Oro Complex at ~226 Ma. This period corresponds to the underplating of the Arenillas-Panupalí unit after the anatectic event.

From the northcentral to the northeastern part of the Celica-Lancones basin, D_4 exhibits a subvertical mylonitic foliation (S_4) (Figure 14b). Most of sigmoidal structures exhibit a top-to-the north direction sense of shear. South of the contact zone between the sediments of the Celica-Lancones basin and the metapelites of the El Tigre unit, the S_4 schistosity increases in intensity within the volcanic series of the Celica-Lancones basin.

At the massif scale, we attribute the large-scale strike swing, the folding of the upper La Bocana unit and the thinning of the Tahuín Group in the central part of the massif to this heterogeneous, Upper Cretaceous compressional event, since they affect all earlier structures.

6. Thermal Modeling of the Triassic Event

6.1. Late Triassic Geometry

The El Oro Complex has experienced several superimposed deformation events (D_1 to D_4), and the geometric and three-dimensional kinematic features related to each event are represented in Figure 8. Whether the D_1 anatectic stage occurred in a regional shear zone during a transpressive tectonic event [*Aspden et al*., 1995], or within a normal sedimentary sequence during an extensional event [*Gabriele*, 2002; *Riel et al*., 2013], has strong implications on the interpretation of the D_2 to D_3 deformational events. *Aspden et al*. [1995] mapped numerous vertical, dextral transpressive faults throughout the Tahuín Group; however, such a fault system has not been observed during the course of this study. Instead, we found that deformation is well distributed all along the massif. Moreover, the southward direction of melt transfer (Figures 11b and 12c), emplacement of the blueschist oceanic unit of Arenillas-Panupalí, and P-T estimates increasing northward throughout the Tahuín Group [*Riel et al*., 2013], support the idea that partial melting occurred within a metasedimentary sequence, that was subsequently tilted.

In order to restore the geometry of the Ecuadorian fore arc during Triassic times, we tilted back the western part of the massif (Figure 15), choosing the western part of the massif as it is the less affected by post D_1 deformational events. In the southwestern part of the massif, the sediments of the Celica-Lancones basin unconformably overlay the Paleozoic sediments of the El Tigre unit (Figure 12a), showing that the main tilting event occurred before the emplacement of the first sediments of the Celica-Lancones basin, i.e., pre-105 Ma [*Jaillard et al*., 1996, 1999]. Consequently, we used an E-W subhorizontal rotation axis that represents the direction of intersection between beddings in Paleozoic and Cretaceous sediments, respectively (Figure 12a). We used a 60° north down rotation angle, which corresponds to the mean planar orientation of the upper

Table 1. Thermal Properties of Used Material

	Thermal Conductivity (Wm − 1/K − 1)	Radiogenic Heat Production (μW/m^3)	Heat Capacity (J/Kg/K)
Metasediments	3.7 [a]	2.0[c]	1000[c]
Granodiorite	3.7 [a]	2.0[c]	1000[c]
Gabbro	2.3 [b]	0.25[c]	1000[c]
Basalt	1.7 [b]	0.25[c]	1000[c]
Mantle	2.9 [b]	0.022[c]	1000[c]

[a] *Taylor et al*. [1986].
[b] *Roy et al*. [1981].
[c] *Turcotte and Schubert* [2002].

migmatitic unit. The results of this restoration and the interpreted geological block diagram of the El Oro metamorphic province during the Triassic are presented in Figure 15. The back-tilted crustal section is about 24 km thick and is characterized by a downward increase in the metamorphic grade (northward on the map). Three major points are noteworthy: (1) the D_1 dominant dextral transpressive shearing, coeval with the migmatitic event, becomes a top-to-the-west extensional shear movement with vertical flattening, (2) the base of the crustal section is characterized by an ~4 km thick gabbroic laccolith intercalated between the Arenillas-Panupalí blueschist oceanic unit and the La Bocana migmatitic unit, (3) the lower crust (continental basement) is lacking below this complete metasedimentary sequence (Tahuín Group).

In the following section, we present the results of a one-dimensional thermal model, which aims at (1) assessing the potential impact of gabbro emplacement [*Aspden et al*., 1995] at crustal root level [*Riel et al*., 2013] as the heat source of the Late Triassic migmatization event and (2) validating the model of rapid cooling of the El Oro Complex as a result of the underplating of the Arenillas-Panupalí blueschist unit [*Gabriele*, 2002; *Riel et al*., 2013].

6.2. Thermal Modeling of the Triassic Anatectic Event

All our models are based on the specific thermal properties of the constitutive lithologies and on the Triassic geometry of the El Oro metamorphic province reconstructed in this paper. As no indicator of significant thinning was recorded during Triassic times [*Riel et al*., 2013], our models are purely thermic and we do not consider heat advection.

6.2.1. Initial Setup

In our one-dimensional models, we used a total thickness of 32 km made from top to bottom of 23 km of metasediments (La Bocana, La Victoria, and El Tigre units) underlain by 4 km of gabbro (Piedras unit) and 5 km of peridotite (underlying mantle). We solved the heat transfer equation (1) derived from the Fourier's law using Gale, a thermomechanical code [*Moresi et al*., 2003].

$$\frac{\partial T}{\partial t} + v \cdot \nabla T = \kappa \nabla^2 T + Q, \tag{1}$$

where T is the temperature, k is the thermal diffusivity, and Q is the radiogenic heat production. Two temperatures for the emplacement of the gabbroic unit were tested: 1100°C and 1300°C, which are the theoretical maximum and minimum temperature values for MORB-derived gabbroic magma [*Kushiro*, 2001]. The temperature of the Marcabeli granodiorite has been set at 800°C [*Castro et al*., 1999]. Following the study of *de Saint Blanquat et al*. [2011], the durations of emplacement of the gabbroic and granodioritic plutons as a function of their volumes have been set at 1 Ma and 0.1 Ma, respectively. The thermal properties used for each material are presented in Table 1. In our models, we do not take into account the effects of the latent heat and melt transfer within the partial melting zone. The effects of the latent heat would buffer and release heat during the prograde and retrograde stages, respectively. Taking into account the latent heat would not significantly change the global shape of the geotherm of the whole crustal section during peak P-T conditions. On the contrary, the effect of melt transfer would significantly change the geotherm shape [*Depine et al*., 2008]. In the La Bocana unit, most of the partially molten volume is controlled by biotite dehydration melting and crystallization of peritectic garnet [*Riel et al*., 2013]. However, the garnet signature is not observed in the rare earth element analyses of the Marcabeli and El Prado plutons [*Aspden et al*., 1995], indicating that melts were not extracted from the unit. This is supported by the fact that melt produced under biotite dehydration

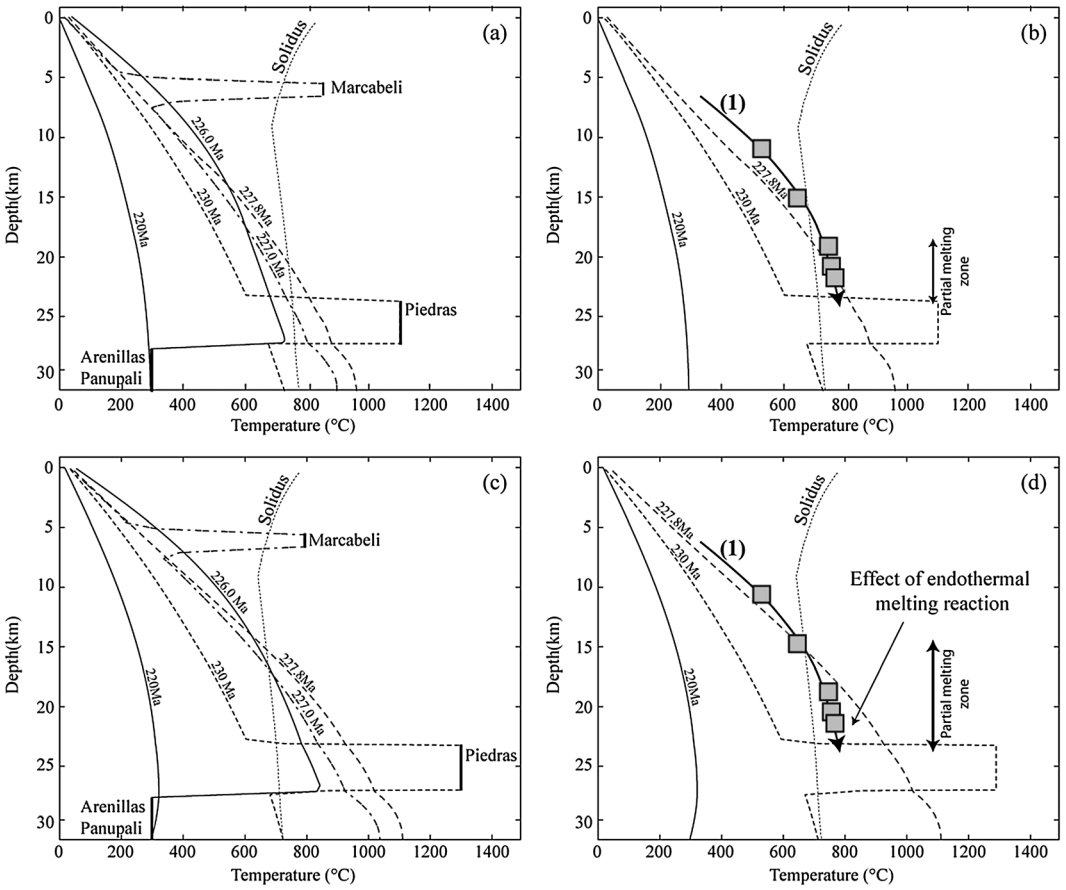

Figure 16. Depth versus Temperature diagram showing the results of thermal modeling of the D_1 Triassic event. (a) Thermal model with a temperature of emplacement of the gabbroic Piedras unit set at 1100°C. (b) Comparison of the obtained results of Figure 16a with the metamorphic gradient at T_{max} of *Riel et al.* [2013]. (c) Thermal model with a temperature of emplacement of the gabbroic Piedras unit set at 1300°C. (d) Comparison of the obtained results of Figure 16c with the metamorphic gradient at T_{max} of *Riel et al.* [2013].

melting has a negative ΔV_r [*Rushmer*, 2001] precluding melt migration until greater fraction of melt are produced, and by the composition of the mesocratic diatexite of the lower La Bocana unit, which does not show a residual composition [*Riel*, 2012]. Therefore, we used a relatively simple diffusive setup in order to reproduce the thermal evolution of the massif.

In our models, the initial crustal geotherm is allowed to equilibrate before the emplacement of the gabbro by imposing a regional ambient temperature of 600°C. The timing of emplacement of the Piedras gabbroic unit is set at ~230 Ma [*Noble et al.*, 1997; *Riel et al.*, 2013] and corresponds to the initial time step T_0. After 1 Ma (229 Ma), the gabbro is allowed to cool down. At 227 Ma, we model the emplacement of the Marcabeli granodiorite between a depth of 5 and 7 km depth (Figure 16) [*Noble et al.*, 1997], using the same thermal properties that are used for the sediments (Table 1), by setting the temperature at 800°C. At 226 Ma, the underplating of the blueschist Arenillas-Panupalí unit is modeled by changing the thermal properties of the 4 km thick peridotitic material to those of subducting basalt and by fixing its initial temperature at 300°C. Consequently the system is allowed to cool down until 220 Ma with a bottom temperature fixed at 300°C.

6.2.2. Thermal Modeling Results

The results of the thermal modeling with gabbro emplaced at an initial temperature of 1100°C show that the maximum vertical extension of the 650°C isotherm is reached at 227.8 Ma (Figure 16a). However, the thickness of the crust exposed to temperature above solidus is limited to 5 km (Figure 16a), which is insufficient compared to the average 10 km thickness of La Bocana migmatitic unit. At 226 Ma, after emplacement of the granodioritic pluton, the upper part of the crust heated up and the geotherm exhibits a more convex shape

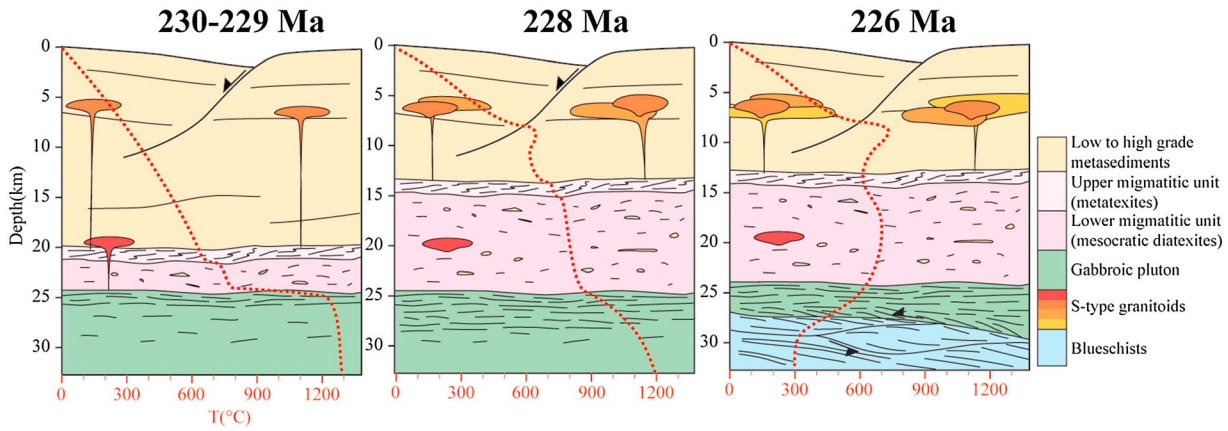

Figure 17. Schematic tectonothermal evolution of the El Oro province during Late Triassic times (230 to 226 Ma). Same color chart as Figures 2 and 3. The geothermal gradient is represented as the red dotted line. The colors from red to yellow of the granitoid intrusion represent the compositional evolution from granodiorite with high contents of basic xenolith, to granite with a low content of basic xenolith.

(Figure 16b). At 226 Ma, underplating of the blueschist Arenillas-Panupalí unit provokes the cooling down of the whole crust section at temperature below 350°C.

For a temperature of emplacement of the gabbroic body at 1300°C, the maximum vertical extension of the isotherm 650°C is also reached at 227.8 Ma (Figures 16c and 16d), with an 8–9 km thickness of crust above the solidus. The calculated geotherm is similar to the estimated geotherm, at least in the upper part of the crustal section (Figure 16d). However, from 15 to 23 km depth, the calculated geotherm exhibits higher temperature. This difference between the estimated and modeled geotherms may be explained by the endothermic reaction of biotite dehydration partial melting [*Thompson and Connolly*, 1995]. At 220 Ma, after underplating of the Arenillas-Panupalí blueschist unit, the whole section has cooled down below 350°C, which is in good agreement with the first K/Ar cooling ages in the La Bocana and La Victoria units at ~220 Ma (Figure 4). Thus, we conclude that the successive emplacement of the Piedras gabbroic unit and the Arenillas-Panupalí blueschist unit between 230 and 226 Ma is consistent with the observed thermal evolution of the El Oro Complex.

7. Discussion

7.1. D_1: Late Triassic Extensional Event

The D_1 deformation represents the main tectonometamorphic event within the El Oro metamorphic province, even if the former shape of the massif has been significantly modified during the D_3 and D_4 deformations. The D_1 deformation is synmigmatitic and associated with the magmatic emplacement of the Piedras gabbroic unit. Moreover, indicators of syntectonic emplacement of the *S*-type Marcabeli granitoid (Figure 11a) show that the D_1 deformation event occurred with magmatic emplacement within the crust. Available ages on the La Bocana migmatites between 230 and 225 Ma (U-Pb method on zircon and monazite) [*Riel et al*., 2013], on the Marcabeli *S*-type granitoid at approximately 227 Ma (U-Pb method on monazite) [*Noble et al*., 1997] and in the Piedras gabbroic unit at 221 ± 17 Ma (U-Pb method on zircon) [*Noble et al*., 1997] imply a Late Triassic age for the D_1 deformation event (230–225 Ma).

The results of thermal modeling and structural study allowed us to reconstruct the tectonothermal evolution of the El Oro metamorphic province during Triassic times (Figure 17).

At ~230 Ma (Figure 17), the emplacement of the Piedras gabbroic unit at high temperature (1300°C) at the base of the crust triggered partial melting of the fore-arc sedimentary succession and the formation of the La Bocana migmatitic unit. The *S*-type granitoid of the La Florida (Figure 5) likely formed during the early stage of anatexis as indicated by its high content of mafic xenoliths. About 2 Ma later, the vertical extent of the partially molten zone was at a maximum and the system started to cool down (Figure 17). During the D_1 stage, extensional, top-to-the west deformation produced heterogeneous deformational structures throughout the lower part of the massif. Related structures were highly dependent on the rheological

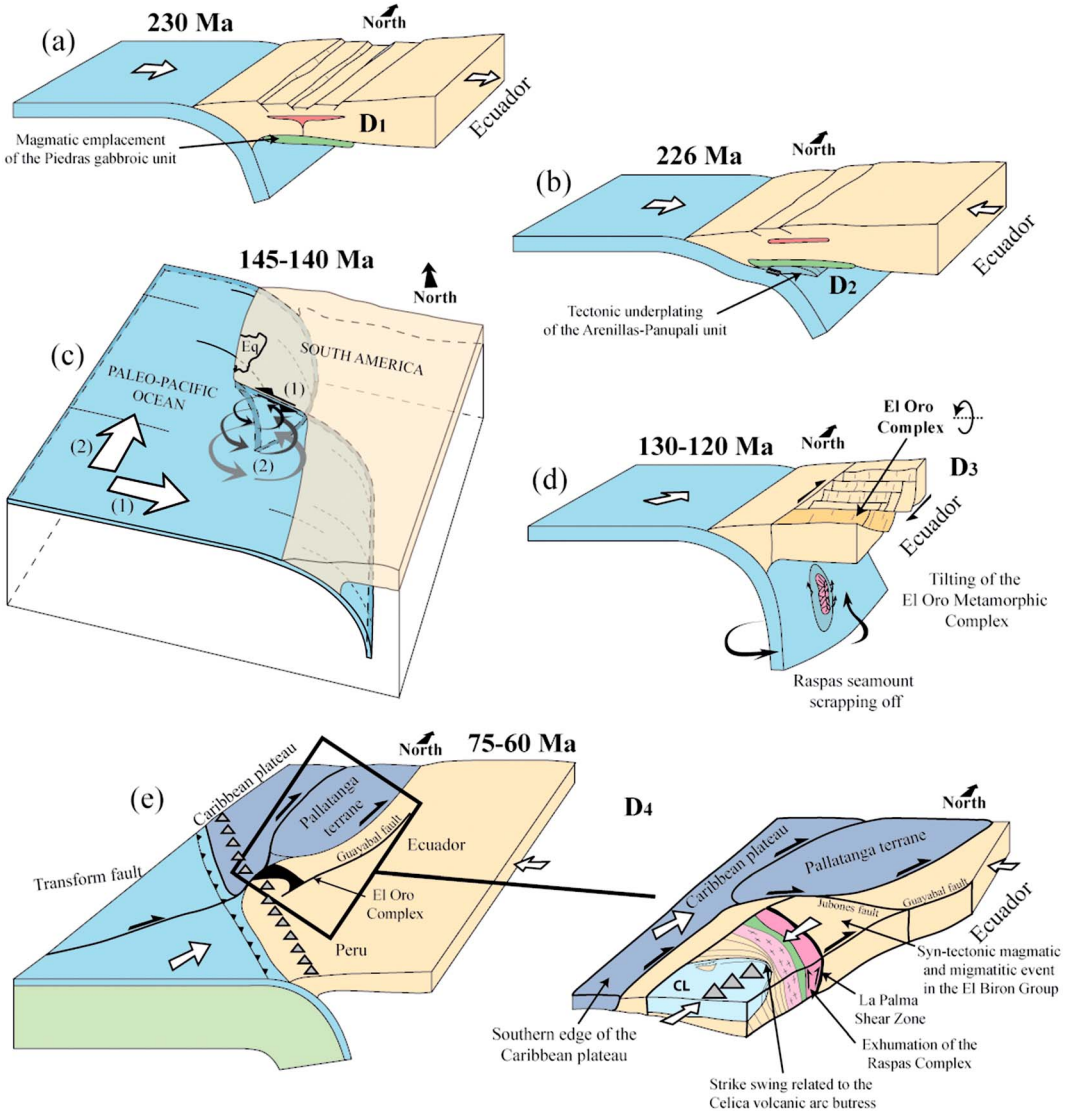

Figure 18. Geodynamical models of the fore-arc zone of southern Ecuador during Mesozoic times. (a) Approximately 230 Ma, magmatic emplacement of the Piedras gabbroic unit in an extensional tectonic setting. (b) Approximately 226 Ma, tectonic underplating of the Arenillas-Panupalí blueschist unit. (c) At 145–140 Ma, arrows 1 and 2 show the change in subduction direction from WSW directed, to NNE directed at 145–140 Ma [*Jaillard et al.*, 1990]. Until 145–140 Ma, the Peruvian margin likely acted as a transform fault, connecting the South American and the Paleopacific upper mantles. When subduction direction changed to NNE directed, the asthenospheric window allowed verticalization of the northern part of the slab by toroidal movements. (d) At 130–120 Ma, the exhumation of the Raspas Ophiolitic Complex at Moho depth level related to slab verticalization. At crustal level, opening of the Celica-Lancones pull-apart basin triggers the tilting of the Birón and El Oro complexes. (e) At 75–60 Ma, accretion of the oceanic terranes against the Ecuadorian margin. The El Oro metamorphic province is compressed between the oceanic terrane and the Celica volcanic arc. The Raspas Ophiolitic Complex is exhumed and we relate the strike swing of the El Oro Complex to the buttressing effect of the Celica arc. At the same time, the Birón Complex undergoes an unconstrained migmatitic event, likely related to the accretion of the oceanic terranes.

properties of the lithologies during the anatectic event. In the upper La Bocana migmatitic unit, the metatexite with low melt content shows contrasting behavior. Leucosome and melanosome were folded together, while quartzitic layers show tensile fractures due to fluid pressure increase controlled by melt displacement (Figure 11b). At the transition zone between the upper and lower parts of the La Bocana unit and in the lower structural levels, the melt content increase, and with convergence viscosities, the shear criteria become rare. In the lower migmatitic unit, the deformation is more "magma-like" and marked by strained xenoliths and folded remnant of quartzitic layers (Figure 6f). Farther east, Lower Triassic ages from

Table 2. Ar/Ar Thermochronological Ages on Amphibole and Phengite in the El Oro Metamorphic Province[a]

Sample	Unit/Lithology	Total Age	Plateau Age	% 39Ar	Intercept Age	40Ar/36Ar	Mean Square Weighted Deviate
97CE1 Amphibole	Raspas/Eclogite	112.4 ± 2.1	114.2 ± 1.6	88,5	113.9 ± 2.5	311 ± 39	3,91
97CE1 Amphibole (bis)	Raspas/Eclogite	127.3 ± 2.0			120.7 ± 4.8	389 ± 74	5,49
97CE3 Phengite	Raspas/Metapelite	121.9 ± 1.1			123.4 ± 1.3	273 ± 11	0,58
97CE4A Amphibole	Raspas/Garnet amphibolite	144.2 ± 4.9			125.5 ± 7.0	312 ± 91	4,58
97CE5 Phengite	Raspas/Metapelite	128.4 ± 1.3	129.3 ± 1.3	86,3	128.8 ± 1.2	302 ± 97	1,88
98RR4 Phengite	Raspas/Eclogite	128.0 ± 1.3	/	/	127.1 ± 1.3	303 ± 13	0,58
98RR4 Amphibole	Raspas/Eclogite	123.2 ± 2.0	117.6 ± 1.8	95,2	116.8 ± 1.4	303 ± 22	0,60
98RR6 Phengite	Raspas/Eclogite	125.3 ± 1.3	/	/	123.9 ± 1.4	297 ± 18	4,42
98TH7 Amphibole	Biron/Amphibolite (gabbro)	113.2 ± 9.1	110.2 ± 10.9	82,2	103.4 ± 1.9	303 ± 11	0,26

[a]See supporting information for details.

acidic intrusive rocks [*Cochrane et al*., 2011] confirm the presence of a belt of Triassic migmatites and *S*-type granites in the arc and back-arc zones. Comparable magmatic events, dated from 260 to approximately 226 Ma on the south American margin, are well known from Northern Colombia [*Restrepo et al*., 2011] to Northern Argentina [*Kay et al*., 1989]. Consequently, the Triassic thermal event, which occurred in a fore-arc position in the El Oro metamorphic complex, is interpreted as the last event of a larger thermal anomaly observed from north Colombia to Chile during Permian-Triassic times (Figure 18a) [*Kay et al*., 1989; *Mišković et al*., 2009; *Riel et al*., 2013].

7.2. D_2: Late Triassic Underplating Event

The D_2 compressional event is restricted to the amphibolitic-facies contact between the oceanic unit of the Arenillas-Panupalí and the Piedras gabbroic unit. S_2 is marked by the development of intrafoliar centimetric folds with a dextral transpressive sense of shear (Figures 12g and 12h). We related the tectonic underplating of the blueschists of the Arenillas-Panupalí unit (Figure 15) under the gabbroic unit of Piedras to this D_2 compressional event. Ar/Ar thermochronology on amphibole in the Piedras unit yielded an age of 226 Ma (Figure 18b)[*Gabriele*, 2002]. We interpret this cooling age as the age of underplating of the oceanic Arenillas-Panupalí unit. Consequently, the El Oro Complex was rapidly cooled down to temperatures $<$350°C as early as 220 Ma [*Aspden et al*., 1995]. A similar event occurred in Colombia, where amphibolitic schists were juxtaposed with Triassic migmatites and granulites during a Late Triassic subduction event [*Bustamante and Juliani*, 2011]. During Triassic times, this kind of tectonomagmatic change of the margin, from extension to compression with waning of the magmatic activity, is also known farther south in Chile and attributed to rapid variations of slab dip [*Gorczyk et al*., 2007].

7.3. D_3: Early Cretaceous Extensional Event

The D_3 extensional event is marked by the mylonitic top-to-the-south contact between the Piedras unit and the La Bocana migmatitic unit (Figures 12e and 12f). We associate this episode with the regional tilting of the whole area (El Oro, Raspas, and Birón Complexes). Based on the E-W trend of the structures of the El Oro Complex and on the later direction of opening of the Celica-Lancones basin [*Jaillard et al*., 1999], tilting likely occurred along an E-W subhorizontal axis and rotated the El Oro Complex up to 60° north down. While *Gabriele* [2002] attributed the tilting of the El Oro metamorphic Complex to an N-S extensional event during Late Triassic times, we found no evidence for such an event. Instead, the main evidence of a tectonic event after Triassic times and before Early Albian times (age of creation of the Celica-Lancones sedimentary basin) are the zircon fission track ages at 137 ± 17 Ma of the Marcabeli Pluton and at 139 ± 10 Ma of the La Victoria unit [*Spikings et al*., 2005], and the Ar/Ar age at 129.5 ± 0.9 Ma on muscovite from the La Palma shear zone [*Gabriele*, 2002]. These ages are identical within error to the age of the peak HP metamorphism of the eclogitic Raspas Complex dated at approximately 130 Ma [*John et al*., 2010], which is followed by a cooling period spanning the 129–117 Ma interval [*Gabriele*, 2002] (Table 2 and the supporting information). These ages are consistent with a phase of extensional tectonics, which triggered both local heating and pluton emplacement and active exhumation of underplated terranes around 130–120 Ma.

In most orogens, periods of exhumation of HP rocks are related to rapid changes in stress conditions [*Guillot et al*., 2009]. In northern South America, the direction of subduction changed from SE to ENE at 145–140 Ma

[*Jaillard et al*., 1990, 2000]. The absence of continuous Jurassic arcs along the NNW trending northern Peru segment suggests that this zone acted as a transform fault during Jurassic times and that Ecuador was located on the southern edge of the subduction zone that occurred along the northern Andes (Figure 18c). We interpret this major change in stress conditions as the triggering event of the exhumation of the Raspas Complex [*Gabriele*, 2002]. Under these conditions, it took approximately 10 Ma to trigger exhumation of the HP rocks. Therefore, we propose that the change in subduction direction from WSW to ENE at ~140 Ma triggered the verticalization of the edge of the slab by toroidal movements (Figure 18c), the exhumation and underplating at a crustal root level of the Raspas ophiolitic Complex (Figure 18d). In this model, verticalization of the slab is made possible due to the occurrence of an asthenospheric window [*Schellart et al*., 2007]. On the base of close radiometric ages, some authors correlated the Raspas Complex with the mafic Arquía HP complex of Colombia, dated at 130–125 Ma [e.g., *Cediel et al*., 2003] or with the Peltetec ophiolites of Ecuador, which yielded plagioclase Ar/Ar ages of 140–130 Ma [*Villagómez and Spikings*, 2013]. However, although the NNE trending Arquía Complex located west of the Colombian Central Cordillera and the NNE trending Peltetec unit located west of the Cordillera of Ecuador actually show a cartographic and structural continuity along the present-day arc zone, the underplated Raspas Complex lies clearly east of this structure and in a fore-arc position. Therefore, in our view, if the common magmatic, structural, and metamorphic history of these units is confirmed, the Arquía Complex and Peltetec unit might be interpreted as exhumed slices of previously underplated ophiolitic units, along a major suture, which bounds the South American continental margin to the west.

Preliminary results on the Birón Complex, north of the ophiolitic Raspas Complex, show that the metamorphic grade increases toward the south from low-grade metasediments to migmatitic rocks, felsic, and mafic plutonic rocks. Although the Birón Complex has been subjected to polyphaze metamorphism and deformation during Triassic to Cretaceous times [*Noble et al*., 1997], its vertical structures and the similarities between its lithologies and those of the Tahuín Group suggest that the Birón Complex and the Tahuín Group belonged to the same fore-arc area before tilting [*Noble et al*., 1997; *Gabriele*, 2002]. Moreover, throughout the El Oro Complex, the increase in pressure conditions within the continental sequences and toward the Raspas ophiolite suggests that tilting occurred around a subhorizontal E-W axis and thus provoked opposite senses of rotation for the Tahuín Group and the Birón Complex, respectively. Since tilting involved the whole tectonic pile of the El Oro Massif, it occurred after the underplating of the Raspas Complex. Deposition of unconformable conglomerates, rich in quartz and metamorphic pebbles, at the base of the mainly volcaniclastic pile of the Celica-Lancones basin suggests that tilting of the El Oro Complex occurred during Early Albian times and was related to the trench-parallel extensional tectonics that created the Celica-Lancones basin [*Jaillard et al*., 1996, 1999]. This interpretation is supported by the age around 110 Ma (Early Albian) obtained from metagabbros from the Birón Complex (Table 1 and the supporting information). Such an Early Cretaceous extensional tectonics is also recorded in Colombia, by the opening of a marginal basin (Quebradagrande Fm) biostratigraphically dated as Valanginian to Albian [*Nivia et al*., 2006] and by a high subsidence and intraplate intrusions in the eastern Cordillera (136–97 Ma) [*Fabre*, 1987; *Vásquez et al*., 2010]. In this view, the D_3 event would comprise the rapid exhumation of the Raspas ophiolitic Complex to crustal root level at approximately 130–120 Ma [*Gabriele*, 2002; *John et al*., 2010] and the tilting of the El Oro Complex at approximately 110 Ma (Figure 18d). Further studies may lead to differentiate these two events.

7.4. D_4: Late Cretaceous-Paleocene Compressional Event

The D_4 event probably includes distinct events and is characterized by a N-S compression and mostly affected the southern and eastern parts of the El Oro Complex and the Celica-Lancones sedimentary basin. On the scale of the massif, the deformation associated with this compressional event is strongly heterogeneous. It was responsible for strike swing within the massif, the regional folding of the Tahuín Group (Figure 8), the final exhumation of the Raspas ophiolitic Complex within the crust [*Gabriele*, 2002], the tilting of the Cretaceous sediments of the northern part of the Celica-Lancones basin, and for a poorly understood tectonothermal event expressed in the Birón Complex by a metagabbroic pluton (73.6 ± 0.5 and 75 ± 0.5 Ma) [*Gabriele*, 2002; *Riel*, 2012], by zircon and apatite fission track ages (68 ± 7 and 61 ± 5 Ma, respectively) on a gneiss [*Spikings et al*., 2005], and by the reactivation of the La Palma shear zone (≈65 Ma) [*Gabriele*, 2002]. In the western part of the massif, D_4 is localized in the sediments of the Celica-Lancones basin and characterized by top-to-the-north thrusting and folding structures. In the eastern part of the massif, between the plutons of Marcabeli and El Prado, the intensity of the compressional D_4 event was maximal and is expressed by the N-S flattening of the

Tahuín Group (Figure 5). To the south, the tectonic contact zone between the El Tigre unit and the Celica-Lancones basin is of tectonic nature and shows a subvertical S_4 schistosity with strong N-S shortening. The age of this tectonic episode is constrained by stratigraphic data from the Celica-Lancones [*Jaillard et al*., 1999], which indicates an important compressional and erosional event from Campanian to Early Paleocene times (≈80–60 Ma) with the development of E-W trending folds with subhorizontal axes [*Jaillard et al*., 1999]. The end of the D_4 compressional event is marked in the Celica-Lancones basin by the unconformable deposition of Late Paleocene sediments [*Jaillard et al*., 1999]. We attribute the strike swing within the massif (Figures 5 and 8) and the heterogeneous deformation associated with the D_4 event to the presence of the Celica arc located in northern Peru to southern Ecuador [*Jaillard et al*., 1996, 1999]. This plutonic belt likely played the role of a buttress focusing the deformation on its northern edge, in the southeastern part of the El Oro complex, while deformation on its sides was more distributed (Figure 18e). At depth, the effect of pinning is likely characterized by the inversion of the dip direction of the foliation south of the lower La Bocana unit (Figures 5 and 8). Moreover, as noticed by *Gabriele* [2002] for the Arenillas-Panupalí unit, the whole El Oro massif can be viewed as an asymmetrical antiform structure centered on the Raspas Complex. We relate this compressional structure to the N-S contraction related to the D_4 deformation event.

Farther east and northeast, *Spikings et al*. [2010] report a 74 ± 0.3 Ma age on biotite in migmatites and an apatite fission track age of 78 ± 9 Ma expressing the exhumation of the Cordillera Real of southern Ecuador. In Ecuador, Late Cretaceous-Paleocene accretions of multiple oceanic plateaus against the margin took place at approximately 75 Ma, 68 Ma, and 58 Ma [*Jaillard et al*., 2004, 2009; *Spikings et al*., 2010]. The first two accretion events coincide with the D_4 event and can account for the compressional deformation observed in the El Oro massif.

In the central Cordillera of the Colombian Andes, Ar/Ar dating on phengites in blueschist-facies rocks yielded ages of 68–62 Ma, interpreted as the timing of exhumation of an oceanic unit, before collision of the Caribbean Plateau with the continental margin [*Bustamante et al*., 2011]. According to *Villagómez and Spikings* [2013], the latter collision is responsible for a period of rapid cooling and exhumation (1.6 km/Ma) between 75 and 65 Ma. Whether the collision of the Caribbean Plateau was preceded by subduction of a marginal sea [*Bourgois et al*., 1987; *Kennan and Pindell*, 2009], allowing the development of localized arc magmatism [*Villagómez et al*., 2011], or occurred through right-lateral docking [*Cediel et al*., 2003; *Jaillard et al*., 2009] is still matter of debate, but is beyond the scope of this paper.

8. Summary and Conclusions

This structural and thermal studies of the El Oro metamorphic province showed that this massif underwent at least four major deformation events from Late Triassic to Paleocene times. During Late Triassic times, at approximately 230 Ma, emplacement of the gabbroic unit of Piedras at a crustal root level triggered partial melting of the fore-arc region in an E-W extensional regime. Throughout the continental sequence, the style of deformation (D_1) is heterogeneous and highly dependent on the P-T conditions and on the proportion of leucosome in the suprasolidus domain. This Triassic anatectic event is interpreted as the last event of a larger thermal anomaly affecting the whole South American margin from Late Permian to Late Triassic times.

At 226 Ma, tectonic underplating of the oceanic blueschists of the Arenillas-Panupalí unit rapidly cooled the Ecuadorian fore arc. Close to the Jurassic-Cretaceous boundary (145–140 Ma), subduction of the Paleopacific plate changed from ESE to NNE directed and 10 Ma later triggered the underplating of the Raspas ophiolitic Complex, likely due to the verticalization of the paleo-Pacific slab (130–120 Ma). During late Early Cretaceous times, trench-parallel extension triggered the opening of the NE-SW trending Celica-Lancones pull-apart Basin in southwest Ecuador (~110 Ma) and tilted the El Oro metamorphic complex more than 90°.

From the Campanian to Maastrichtian (80–65 Ma), extension switched to N-S directed compression, most probably related to the accretion of oceanic terranes both in Ecuador and Colombia. The Celica volcanic arc acted as a buttress and heterogeneously deformed the El Oro metamorphic province, creating the present-day regional strike swing and the antiform structure at the massif scale. At the same time in the Birón Complex, a localized and poorly constrained HT event overprinted previous structures.

Our work, which combines field observations, structural interpretation, and thermal modeling, shows that the El Oro metamorphic province underwent multiple events of HP rock underplating and HT metamorphism

associated with *S*-type magmatism. Therefore, the behavior of fore-arc regions seems to have been oversimplified in the last few decades. Moreover, the migmatitic nature of the La Bocana unit shows that almost half of the thickness of the fore-arc region (~10 km) has been subjected to partial melting during Late Triassic times, leading to textural and chemical differentiation of a metasedimentary sequence into a newly formed lower crust.

Acknowledgments
Data supporting Table 2 are available as in the supporting information. This research was funded by the SEDIT project (INSU, 2008–2009). We thank the IRD–Quito for logistical support during the 2008 and 2010 field campaigns. We kindly thank David Chew, Michael Gazley, Jacques Bourgois, and the Associate Editor, Paola Vannucchi, for their helpful reviews.

References

Aspden, J. A., S. H. Harrison, and C. C. Rundle (1992), New geochronological control for the tectonomagmatic evolution of the metamorphic basement, cordillera real and El–Oro province of Ecuador, *J. South Am. Earth Sci.*, *6*, 77–96.

Aspden, J. A., W. Bonilla, and P. Duque (1995), *The El Oro Metamorphic Complex, Ecuador: Geology and Economic Mineral Deposits*, *Overseas Geol. Miner. Resour.*, vol. 67, 63 pp., British Geol. Surv. Publ., Keyworth, Nottingham, England.

Bosch, D., P. Gabriele, H. Lapierre, J.-L. Malfere, and E. Jaillard (2002), Geodynamic significance of the Raspas Metamorphic Complex (SW Ecuador): Geochemical and isotopic constraints, *Tectonophysics*, *345*, 83–102.

Bourgois, J., J.-F. Toussaint, H. González, J. Azema, B. Calle, A. Desmet, A. Murcia, A. Acevedo, E. Parra, and J. Tournon (1987), Geological history of the Cretaceous ophiolitic complexes of Northwestern South America (Colombian Andes), *Tectonophysics*, *143*, 307–327.

Bustamante, A., and C. Juliani (2011), Unraveling an antique subduction process from metamorphic basement around Medellín city, Central Cordillera of Colombian Andes, *J. South Am. Earth Sci.*, *32*, 210–221.

Bustamante, A., C. Juliani, C. M. Hall, and E. J. Essene (2011), 40Ar/39Ar ages from blueschists of the Jambaló region, Central Cordillera of Colombia: Implications on the styles of accretion in the Northern Andes, *Geol. Acta*, *9*, 351–362.

Castro, A., A. E. Patiño Douce, L. G. Corretgé, J. D. de la Rosa, M. El-Biad, and H. El-Hmidi (1999), Origin of peraluminous granites and granodiorites, Iberian massif, Spain: An experimental test of granite petrogenesis, *Contrib. Mineral. Petrol.*, *135*, 255–276.

Cediel, F., R. P. Shaw, and C. Cáceres (2003), Tectonic assembly of the Northern Andean Block, in *The Circum-Gulf of Mexico and Caribbean: Hydrocarbon Habitats, Basin Formation and Plate Tectonics*, edited by C. Bartolini, R. T. Buffler, and J. Blickwede, *Mem. Am. Assoc. Pet. Geol.*, *79*, 815–848.

Chew, D. M., U. Schaltegger, J. Košler, M. J. Whitehouse, M. Gutjahr, R. A. Spikings, and A. Miškovìc (2007), U-Pb geochronologic evidence for the evolution of the Gondwanan margin of the north-central Andes, *Geol. Soc. Am. Bull.*, *119*, 697–711.

Chew, D. M., T. Magna, C. L. Kirkland, A. Miskovic, A. Cardona, R. Spikings, and U. Schaltegger (2008), Detrital zircon fingerprint of the Proto-Andes: Evidence for a Neoproterozoic active margin?, *Precambrian Res.*, *167*, 186–200.

Cochrane, R., R. Spikings, W. Winkler, A. Ulianov, and M. Chiaradia (2011), Triassic to Early Cretaceous tectonic evolution of Ecuador: Insights from U–Pb LA–ICP–MS geochronology, geochemistry and provenance studies, Geophys. Res. Abstract 13, EGU2011–2650–2.

Depine, G. V., C. L. Andronicos, and J. Phipps-Morgan (2008), Near-isothermal conditions in the middle and lower crust induced by melt migration, *Nature*, *452*, 80–83.

de Saint Blanquat, M., E. Horsman, G. Habert, S. Morgan, O. Vanderhaeghe, R. Law, and B. Tikoff (2011), Multiscale magmatic cyclicity, duration of pluton construction, and the paradoxical relationship between tectonism and plutonism in continental arcs, *Tectonophysics*, *500*, 20–33.

Fabre, A. (1987), Tectonique et génération d'hydrocarbures: Un modèle de l'évolution de la Cordillère Orientale de Colombie et du Bassin des Llanos pendant le Crétacé et le Tertiaire, *Arch. Sci. Genève*, *40*, 145–190.

Feininger, T. (1978), *Geologic Map of Western El Oro Province*, Escuela Politecnica Nacional, Quito, Ecuador.

Feininger, T., and M. L. Silberman (1982), K–Ar geochronology of basement rocks on the Northern Flank of the Huancabamba deflection, Ecuador, *U.S. Geol. Surv. Open File Rep.*, 82–206.

Gabriele, P. (2002), HP terranes exhumation in an active margin setting: Geology, petrology and geochemistry of the Raspas Complex in SW Ecuador, Unpublished PhD Thesis, Univ. of Lausanne, Switzerland.

Gabriele, P., M. Ballèvre, E. Jaillard, and J. Hernandez (2003), Garnet–chloritoid–kyanite metapelites from the Raspas Complex (SW Ecuador): A key eclogite–facies assemblage, *Eur. J. Mineral.*, *15*, 977–989.

Gorczyk, W., A. P. Willner, T. V. Gerya, J. A. D. Connolly, and J.-P. Burg (2007), Physical controls of magmatic productivity at Pacific-type convergent margins: Numerical modeling, *Phys. Earth Planet. Inter.*, *163*, 209–232.

Guillot, S., K. Hattori, P. Agard, S. Schwartz, and O. Vidal (2009), Exhumation processes in oceanic and continental subduction contexts: A review, in *Subduction Zone Dynamics*, edited by S. Lallemand and F. Funiciello, pp. 175–204, Springer, Berlin, Heidelberg.

Jaillard, E., P. Soler, G. Carlier, and T. Mourier (1990), Geodynamic evolution of the Northern and Central Andes during early - middle Mesozoic times: A Tethyan model, *J. Geol. Soc. London*, *147*, 1009–1022.

Jaillard, E., M. Ordoñez, P. Bengtson, G. Berrones, M. Bonhomme, N. Jiménez, and I. Zambrano (1996), Sedimentary and tectonic evolution of the arc zone of southwestern Ecuador during Late Cretaceous and Early Tertiary times, *J. South Am. Earth Sci.*, *9*, 131–140.

Jaillard, E., G. Laubacher, P. Bengtson, A. V. Dhondt, and L. G. Bulot (1999), Stratigraphy and evolution of the forearc "Celica–Lancones Basin" of Southwestern Ecuador, *J. South Am. Earth Sci.*, *12*, 51–68.

Jaillard, E., G. Hérail, T. Monfret, E. Díaz-Martínez, P. Baby, A. Lavenu, and J.-F. Dumont (2000), Tectonic evolution of the Andes of Ecuador, Peru, Bolivia and northernmost Chile, in *Tectonic Evolution of South America, 31st International Geological Congress*, edited by U. G. Cordani et al., pp. 481–559, Rio de Janeiro, Brazil.

Jaillard, E., M. Ordoñez, J. Suárez, J. Toro, D. Iza, and W. Lugo (2004), Stratigraphy of the Late Cretaceous-Paleogene deposits of the Western Cordillera of Central Ecuador: Geodynamic implications, *J. South Am. Earth Sci.*, *17*, 49–58.

Jaillard, E., H. Lapierre, M. Ordoñez, J. T. Álava, A. Amórtegui, and J. Vanmelle (2009), Accreted oceanic terranes in Ecuador: Southern edge of the Caribbean Plate?, in *The Origin and Evolution of the Caribbean Plate*, edited by K. James, M. A. Lorente, and J. Pindell, *Geol. Soc. London Spec. Publ.*, *328*, 467–483.

John, T., E. E. Scherer, V. Schenk, P. Herms, R. Halama, and D. Garbe-Schönberg (2010), Subducted seamounts in an eclogite–facies ophiolite sequence: The Andean Raspas Complex, SW Ecuador, *Contrib. Mineral. Petrol.*, *159*, 265–284.

Kay, S. M., V. A. Ramos, C. Mpodozis, and P. Sruoga (1989), Late Paleozoic to Jurassic silicic magmatism at the Gondwana margin: Analogy to the Middle Proterozoic in North America?, *Geology*, *17*, 324–328.

Kennan, L., and J. L. Pindell (2009), Dextral shear, terrane accretion and basin formation in the Northern Andes: Best explained by interaction with a Pacific-derived Caribbean plate?, in *The Origin and Evolution of the Caribbean Plate*., edited by K. James, M. A. Lorente, and J. Pindell, *Geol. Soc. London Spec. Publ.*, *328*, 487–531.

Kushiro, I. (2001), Partial melting experiments on peridotites and origin of mid-ocean ridge basalt, *Annu. Rev. Earth Planet. Sci.*, *29*, 71–107.
Martínez, M. (1970), Geología del basamento Paleozóico en las Montañas de Amotape y posible origen del petróleo en las rocas Paleozóicas del noreste de Perú, *Primer Congr. Latinoam. Geol.*, *2*, 105–138.
Mišković, A., U. Schaltegger, R. A. Spikings, D. M. Chew, and J. Košler (2009), Tectono–magmatic evolution of Western Amazonia: Geochemical characterisation and zircon U–Pb geochronologic constraints from the Peruvian Eastern Cordilleran granitoids, *Geol. Soc. Am. Bull.*, *121*, 1289–1324.
Moresi, L. N., F. Dufour, and H.-B. Mühlhaus (2003), A Lagrangian integration point finite element method for large deformation modeling of viscoelastic geomaterials, *J. Comput. Phys.*, *184*, 476–497.
Nivia, A., G. F. Marriner, A. C. Kerr, and J. Tarney (2006), The Quebradagrande Complex: A Loweer Cretaceous ensialic marginal basin in the Central Cordillera of the Colombian Andes, *J. South Am. Earth Sci.*, *21*, 423–436.
Noble, S. R., J. A. Aspden, and R. Jemielita (1997), Northern Andean crustal evolution: New U–Pb geochronological constraints from Ecuador, *Geol. Soc. Am. Bull.*, *109*, 789–798.
Restrepo, J. J., O. Ordóñez-Carmona, R. Armstrong, and M. M. Pimentel (2011), Triassic metamorphism in the northern part of the Tahamí Terrane of the central cordillera of Colombia, *J. South Am. Earth Sci.*, *32*, 497–507.
Riel, N. (2012), Anomalie thermique et sous–placage en zone d'avant–arc:exemple du massif triasique de El Oro, Equateur, PhD thesis, pp. 364, Univ. of Grenoble, Grenoble, France.
Riel, N., et al. (2013), A metamorphic and geochronogical study of the Triassic El Oro metamorphic Complex in Ecuador: Implications for high–temperature metamorphism in a forearc zone, *Lithos*, *156-159*, 41–68, doi:10.1016/j.lithos.2012.10.005.
Roy, R. F., A. E. Beck, and Y. S. Touloukian (1981), Thermophysical Properties of Rocks, in *Physical Properties of Rocks and Minerals*, edited by Y. S. Touloukian, W. R. Judd, and R. F. Roy, pp. 409–502, Mc Graw-Hill, New York.
Rushmer, T. (2001), Volume change during partial melting reactions: Implications for melt extraction, melt geochemistry and crustal rheology, *Tectonophysics*, *342*, 389–405.
Schellart, W. P., J. Freeman, D. R. Stegman, L. Moresi, and D. May (2007), Evolution and diversity of subduction zones controlled by slab width, *Nature*, *446*, 308–311.
Spikings, R. A., W. Winkler, R. A. Hughes, and R. Handler (2005), Thermochronology of Allochthonous Terranes in Ecuador: Unraveling the accretionary and post-accretionary history of the Northern Andes, *Tectonophysics*, *399*, 195–220.
Spikings, R. A., P. V. Crowhurst, W. Winkler, and D. Villagómez (2010), Syn- and post-accretionary cooling history of the Ecuadorian Andes constrained by their in situ and detrital thermochronometric record, *J. South Am. Earth Sci.*, *30*, 121–133.
Taylor, A. E., A. Judge, and V. Allen (1986), Terrestrial heat flow from Project Cesar, Alpha Ridge, Arctic Ocean, *J. Geodyn.*, *6*, 137–76.
Thompson, A. B., and J. A. D. Connolly (1995), Melting of the continental crust; some thermal and petrological constraints on anatexis in continental collision zones and other tectonic settings, *J. Geophys. Res.*, *100*, 15,565–15,579, doi:10.1029/95JB00191.
Turcotte, D. L., and G. Schubert (2002), *Geodynamics – Applications of Continuum Physics to Geological Problems*, 450 pp., John Wiley, New York.
Vásquez, M., U. Altenberger, R. L. Romer, M. Sudo, and J. M. Moreno-Murillo (2010), Magmatic evolution of the Andean Eastern Cordillera of Colombia during the Cretaceous: Influence of previous tectonic processes, *J. South Am. Earth Sci.*, *29*, 171–186.
Villagómez, D., and R. Spikings (2013), Thermochronology and tectonics of the Central and Western Cordilleras of Colombia: Early Cretaceous-Tertiary evolution of the Northern Andes, *Lithos*, *160-161*, 228–249.
Villagómez, D., R. Spikings, T. Magna, A. Kammer, W. Winkler, and A. Beltrán (2011), Geochronology, geochemistry and tectonic evolution of the Western and Central cordilleras of Colombia, *Lithos*, *125*, 875–896.